Articles

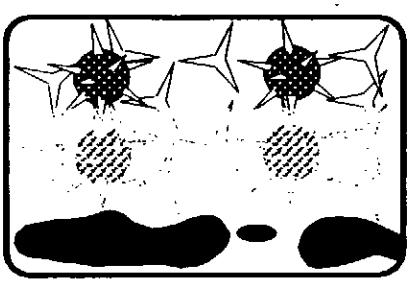

Diagenesis #13. Origin of chert: Diagenesis of biogenic siliceous sediments

Reinhard Hesse
Department of Geological Sciences
McGill University
3450 University Street
Montreal, Quebec H3A 2A7

[Editor's note: This article is a companion to Hesse *(in press)*. Both articles will be published in Geoscience Canada Reprint Series 4, *Diagenesis*.]

Introduction

Highly silicified sedimentary rocks are generally called chert, but are also known under generic or local names such as radiolarite, porcelanite, flint, jasper, lydite, or novaculite. They may contain up to 95% or more silica. The origin of chert has been much debated in the past. Systematic studies in the last decade have advanced our knowledge of chert genesis significantly and have shed light on many facets of the so-called "chert-problem". The three basic aspects of the chert-problem, which are (1) the source of the silica, (2) the depositional environment of siliceous sediments and (3) the diagenesis of cherts and chert-bearing rocks are now understood in principle. Nevertheless, a historical perspective will be included in this review in order to give the reader some idea of the developments that led to our present understanding of silica diagenesis and to the problems on which current research is focussed. Although the emphasis of this review is on diagenesis, a brief outline of the first two aspects of the former chert-problem will be presented in the introductory sections because a discussion of silica diagenesis is not possible without frequent reference to these other subjects.

Terminology and concentration units for dissolved and solid SiO_2 phases and fine-grained siliceous sediments. To facilitate communication, a few of the terms and concentration units used for the various dissolved and solid species of SiO_2 as well as for fine-grained siliceous sediments will be defined at the outset:

Dissolved silicon (or simply *silicon*) is the term used for the undissociated monomeric silicic acid $Si(OH)_4$ which is the dominant species of dissolved SiO_2 in most natural waters. Its anhydrous equivalent SiO_2 has a molecular weight of about 60. One ppm SiO_2 by weight (or 1 $mg \cdot kg^{-1}$) therefore corresponds to 16.6 microgram-atoms SiO_2 per litre ($\mu g\text{-at} \cdot L^{-1}$, the concentration unit commonly used in the oceanographic literature) or 16.6 μM (where μM stands for micromole per litre). This in turn is equivalent to 0.467 $mg \cdot L^{-1}$ Si. Conversely, 1 mM (= 1 millimole per litre) corresponds to 60 ppm SiO_2.

In its various solid phases, SiO_2 will be referred to as *silica*. These include amorphous silica or opal-A, cristobalite-tridymite or opal-CT, low-temperature cristobalite or opal-C, low-temperature tridymite, chalcedony, quartzine, lutecite and quartz. Physical and mineralogical characteristics of these species are discussed in appropriate sections of the paper.

Biogenic fine-grained siliceous sediments are called *siliceous oozes*. The term *"siliceous mud"* instead of ooze is used for those deposits which have a substantial detrital terrigenous component. *Diatom ooze*, *radiolarian ooze* and (sponge) *spicule ooze* are distinguished according to the main groups of organisms contributing siliceous shells to pelagic (or lacustrine) sediments. Their lithified equivalents are *diatomite*, *radiolarite* and *spiculite*. The rock names porcelanite and chert are used to denote fine-grained siliceous sedimentary rocks according to their textural and physical properties. *"Porcelanite"* refers to a porous rock with dull or matte lustre similar to unglazed porcelain whereas *"chert"* denotes a dense vitreous, hard and brittle rock (Bramlette, 1946). The difference between the two is related to detrital content, especially clay content, which is higher (25-50%) in porcelanite than in chert (0-25%, Jones and Murchey, 1986). Siliceous rocks with more than 50% clay are called siliceous claystone, mudstone, or argillite. *Lydite* is a dark-grey to black variety of argillaceous chert or siliceous argillite. Local names for various chert types include flint, jasper, and novaculite. *Flint* is a name widely applied to chert nodules in the Upper Cretaceous chalk of northwestern Europe (Schmid, 1986), which have been used in artifacts and tools made by early man (arrowheads, knives, drills, *etc.*). The term is synonymous with firestone or hornstone and has been applied in the common language in England for more than a thousand years to any very hard and dense rock with conchoidal fracture surfaces (Bates and Jackson, 1980). Generally, *jasper* is a red, brown or yellow variety of chert (also green or black) that derives its colour from iron-oxide impurities. It may be associated with iron-ores or soil-forming processes. *Novaculite* is very dense, light-coloured quartz-chert from the Ouachita Mountains in Arkansas and Oklahoma, which has undergone high-grade diagenesis and low- to intermediate-grade metamorphism. The word is derived from the Latin word for razor (*novacula*) and has been formerly used in England for rocks that served as whetstones or razor hones (Goldstein, 1959).

Sources of Non-detrital Silica in Siliceous Sediments

There are three main sources of non-detrital silica in sediments: (i) siliceous tests and skeletal elements of organisms, (ii) weathering solutions in semi-arid climates, and (iii) silicon supplied in solution by hydrothermal-volcanic systems. The predominant source of Phanerozoic cherts is biogenic, although there also exist hydrothermal-volcanogenic deposits or low-temperature chemogenic deposits (in alkaline lakes or arid to semi-arid soils). In the Precambrian, the cherty variety of banded iron formations represents a widespread type of chert almost unknown from younger geologic periods whose origin is still being debated. Low-

temperature chemogenic and/or hydrothermal-volcanogenic deposits are the dominant Precambrian types of chert. This review focusses on the diagenesis of biogenic siliceous sediments, whereas another review (Hesse, *in press*) deals with other chert types.

The total present-day silica production by marine organisms such as diatoms, radiolarians, silicoflagellates or siliceous sponges is estimated at 2.5×10^{16} grams per annum ($g \cdot a^{-1}$) or about 25 times the input of silica to the oceans ($10.8 \times 10^{14}\ g \cdot a^{-1}$), to which rivers contribute 4.3, pore-water reflux a potential 5.7, submarine weathering 0.8, and submarine volcanism $0.05 \times 10^{14}\ g \cdot a^{-1}$, according to Heath (1974). More recent calculations by Edmond *et al.* (1979a) attribute an additional $1.9 \times 10^{14}\ g \cdot a^{-1}$ to hydrothermal influx, although this still would not balance input and output. The greater part of the output is primary production by diatoms which appear at the beginning of the marine food chain. The discrepancy between the figures for input and output, however, is not a real difference because of internal oceanic recycling which involves dissolution of siliceous tests and upwelling of the dissolved silica (Figure 1). According to estimates by different authors (*e.g.*, Calvert, 1968; Berger, 1970; Hurd, 1973) between 90 and 99% of the silica extracted from surface seawater by shell-producing organisms (in the form of solid amorphous silica) redissolves before burial. Dissolution starts after death of the organisms when the tests settle through the water column, and continues while they rest on the sea floor, and particularly after burial in the sediment. A fraction of the silica dissolved during burial, however, returns to the ocean by means of diffusion. This is evident from the strong silica concentration gradient in the upper 20 cm of the sediment. DeMaster (1981) includes the figure for pore-water reflux quoted above ($5.7 \times 10^{14}\ g \cdot a^{-1}$) with internal oceanic recycling. This is the diffusional flux across the sediment/water interface. Most of the dissolution during burial, however, provides the silicon required for diagenetic reprecipitation in the sediment, the mechanisms of which are the central topic of this review.

Depositional Environments of Siliceous Sediments

Biogenic siliceous oozes on the modern ocean floors. Biogenic siliceous sediments occur both in deep and shallow-water depositional environments. Siliceous ooze is a typical pelagic sediment which accumulates on the deep-sea floor in regions where silica production in surface waters is high. This is the case in zones of oceanic upwelling, where nutrients dissolved somewhere at depth in the oceans are returned to the surface. Upwelling is related to global or local oceanic circulation patterns and occurs (i) along equatorial divergences, (ii) in the vicinity of subpolar convergences, (iii) along the west coasts of continents, and (iv) in certain marginal seas where surface currents diverge or are driven offshore. In the Pacific Ocean, regions of upwelling correspond to 5 major belts of silica accumulation on the sea floor (Figure 2): an equatorial belt (north of the equator), the sub-Antarctic belt (north of the Antarctic convergence), the sub-Arctic belt (south of the Arctic convergence), the Gulf of California (continental west coast/marginal sea upwelling) and the Okhotsk and Bering Seas (marginal sea setting).

In low-latitude areas of high primary surface production, pelagic carbonates are deposited together with siliceous tests leading to mixed calcareous-siliceous oozes. Pure siliceous ooze or high-silica ooze will only accumulate in areas where dilution by other components is inhibited or decreased. This is the case below the calcite compensation level (CCL), *e.g.*, in the equatorial belt of siliceous oozes to the north of the mixed calcareous-siliceous belt. (An equivalent belt south of the equator does not exist, because the young, shallow oceanic crust has not yet subsided below the CCL). Temperature affects silica solubility more than pressure. Silica is therefore considerably more soluble in surface waters than at great depth (Figure 3). In the deep sea, below 1 or 2 km water depth, temperature decreases only a few degrees Celsius. The temperature effect thus becomes very small and can be offset by the effect of increasing pressure which raises silica solubility. Pressure-corrected curves for silica solubility (Figure 3) therefore have a minimum at about 1.5 km depth, below which solubility increases slightly. However, an equivalent of the CCL for silica has not been observed in the oceans. From the foregoing it follows that silica dissolution is predominant in the upper 1,000 m of the water column, in contrast with the dissolution of pelagic carbonates. In the Gulf of California, siliceous muds accumulate despite the supply or terrigenous detritus to the gulf, because the terrigenous input is seasonally and locally suppressed by the prevailing wind and current patterns (Calvert, 1966a,b).

Pelagic stratigraphy. The zonal distribution of pelagic sediments as described for the Pacific, when combined with plate motions and the thermal subsidence of ageing oceanic crust, gives rise to a distinct stratigraphic succession of pelagic sediments, the so-called "plate stratigraphy" (Berger and Winterer, 1974) or the "pelagic" stratigraphy described by Hesse *et al.* (1974). It is typically developed on Cretaceous-Cenozoic crust of the major oceans and consists (from bottom to top) of mid-ocean ridge basalt overlain by pelagic carbonates, then cherts and siliceous oozes and brown abyssal clay (Figure 4). Calcareous ooze is generally the first pelagic sediment deposited on newly created oceanic crust, at least since Late Jurassic time, because young oceanic crust at the crest of mid-ocean ridges is elevated and normally projects above the CCL. With age-related subsidence, the crust will eventually pass below the CCL, leading to the deposition of siliceous ooze and/or brown abyssal clay. In the Pacific, the sequence may be duplicated, if the northwestward motion of the Pacific plate carries it under the equator, where the CCL is depressed sufficiently to intercept the sea floor for a second time (Figure 4). Upon approaching the West and North Pacific island arc/deep-sea trench systems, the oceanic crustal section which carries this pelagic stratigraphy, collects an ultimate cap of hemipelagic and volcanogenic sediments before its history is terminated in a subduction zone. During subduction, some of the pelagic sediments may be scraped from the

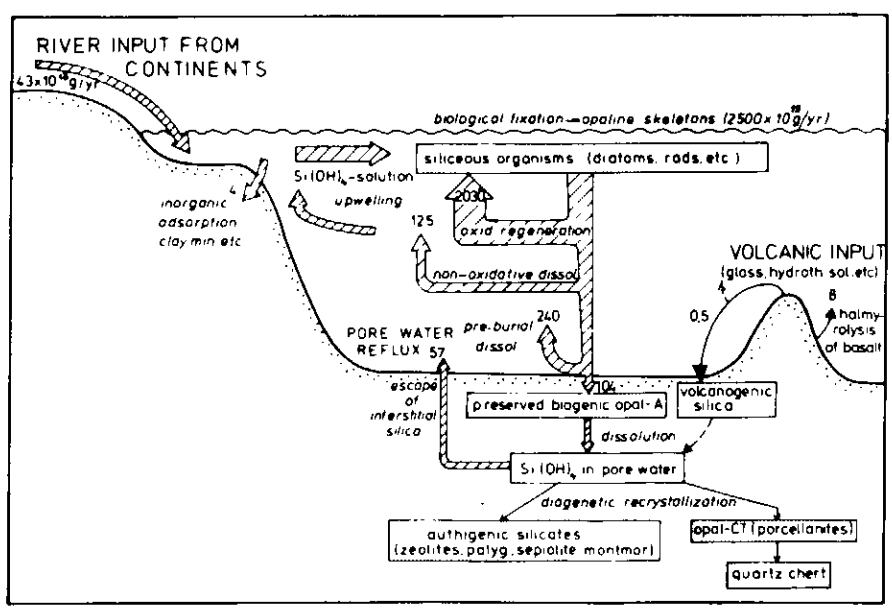

Figure 1 *Global dissolved silicon budget of the oceans. (From Riech and v. Rad, 1979, modified after Heath, 1974). All numbers are in 10^{13}g SiO_2 per annum*

downgoing crustal slab and incorporated into an imbricate tectonic wedge under the trench-slope and forearc basin by tectonic accretion. In this way, some siliceous deposits escape subduction and may ultimately be returned to the surface by tectonic uplift in orogenic belts, where they may occur as parts of ophiolite sequences (see next paragraph).

Ophiolites, the "Steinmann trinity", and chert in mountain belts. In the plate-stratigraphic succession, siliceous sediments typically occupy an intermediate position between pelagic carbonate and brown abyssal clay. In mountain belts, the association of radiolarian cherts in an ordered sequence with other pelagic sediments and with mafic and ultramafic rocks of the ophiolite suite has been recognized for nearly a century. In the Alps, it was called the "Steinmann trinity", after its discoverer Gustav Steinmann (1906, 1927). It was taken as a suite of rocks diagnostic for "eugeosynclines", whose equivalence with oceanic crust was only recognized with the advent of the plate tectonics concept (*e.g.*, Chipping, 1971). Ophiolites and the Steinmann trinity

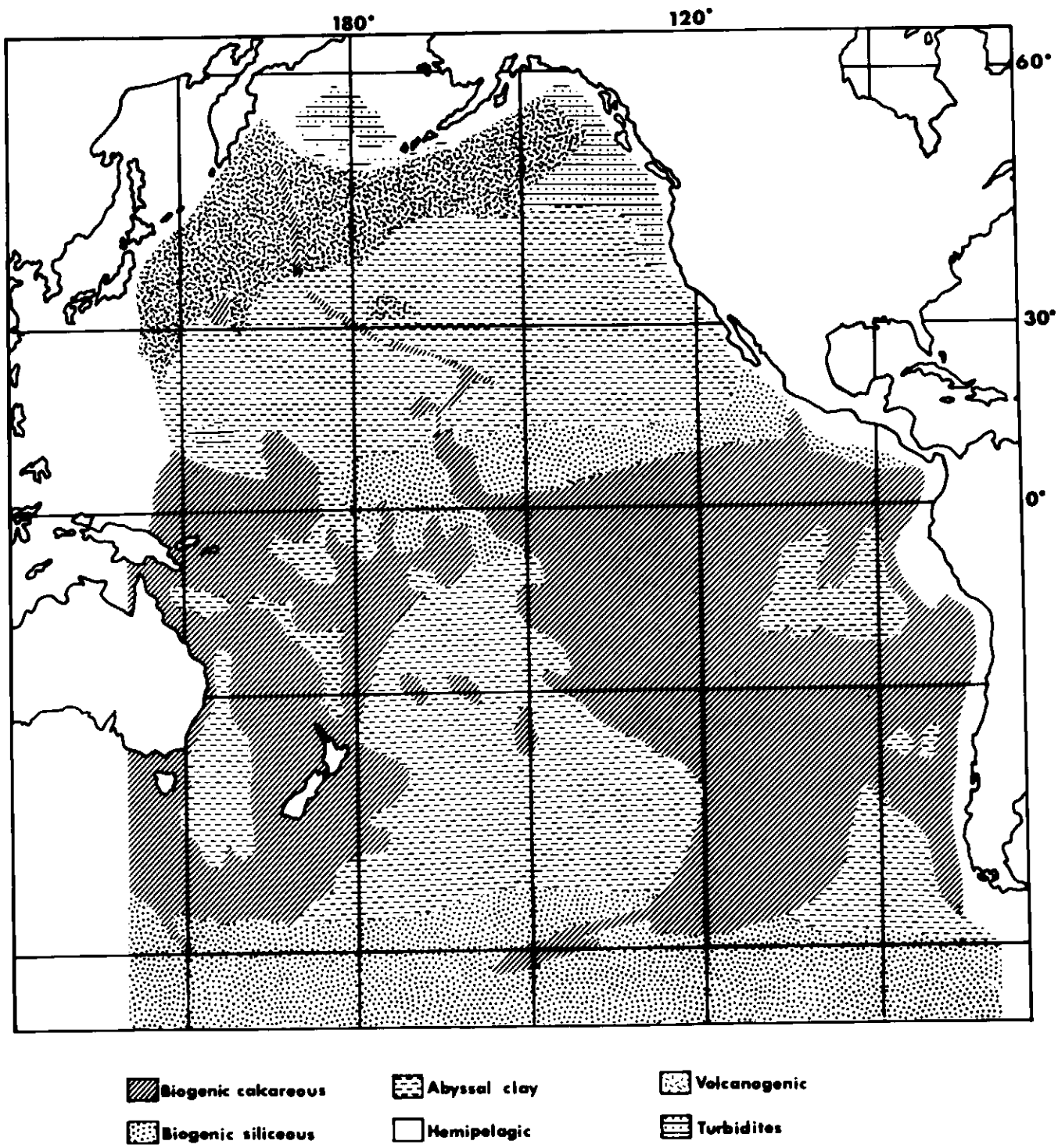

Figure 2 *Distribution of pelagic sediment types in the bottom sediments of the Pacific Ocean (from Hesse* et al., *1974). Note that siliceous sediments south of the Aleutian and Kurile Islands are mixed with volcanogenic material.*

are thus today identified with the remnants of oceanic crust and mantle in mountain belts (Figure 5). The "petrogenetic problem", which Wenk (1949) saw in the association of ultrasiliceous sediments (radiolarites) with ultrabasic igneous rocks, is no longer a problem. The silica of the siliceous pelagic sediments is not derived directly from silica-undersaturated basic and ultrabasic rocks by submarine exhalative volcanism, as previously thought (as recently as 1971: *see* Gibson and Towe, 1971), but through upwelling from the oceanic silica reservoir and biogenic precipitation in surface waters, as discussed above. The "geotectonic significance" of chert, where it forms part of an ophiolite sequence, is not affected by this reinterpretation. However, since the distribution of siliceous sediments and cherts is controlled by (paleo-)oceanographic conditions, they are therefore not restricted to oceanic crust. It is no surprise to find ancient cherts underlain by continental crust as, for example in the Apennines (McBride and Folk, 1979), where they occur next to ophiolitic cherts (Folk and McBride, 1978). It should also be mentioned that in the Alpine – Mediterranean ophiolite terrains, the sequence "pelagic carbonate – chert – red abyssal shale" is generally reversed compared with the standard sequence found in the Pacific, with radiolarian cherts preceding the pelagic carbonates. This is probably due to a much shallower CCL in pre-Late Jurassic oceans, a consequence of the absence of widespread calcareous planktonic organisms in these times (Bosellini and Winterer, 1975). Although most ophiolite-associated cherts are not volcanogenic, but biogenic, in origin, as we know now, the geochemistry of some radiolarian cherts nevertheless reveals a metasomatic overprint which is due to igneous activity at a former mid-ocean ridge. Examples are the Jurassic Mediterranean bedded cherts just mentioned which directly overlie basalt of the oceanic crust. Their upward decreasing iron content and increasing manganese concentration with increasing stratigraphic distance from the basalt reflects the effects of hydrothermal fluid circulation in the sediments (Barrett, 1981).

Formation of bedded chert. Many ancient, bedded chert formations for which geological and sedimentological evidence suggests a deep-water origin, appear to owe their emplacement to redeposition of siliceous pelagic sediment by turbidity currents (*e.g.*, Imoto and Saito, 1973; Nisbet and Price, 1974; Robertson, 1977; McBride and Folk, 1979) or other ocean currents. Sedimentary structures and fabrics, such as flute casts and other sole marks (*e.g.*, Imoto *et al.*, 1974), common graded bedding, parallel lamination, faint cross lamination, starved ripples, grain fabrics such as parallel alignment of sponge spicules and radiolarians, shale clasts, and sharp contacts with interbedded shales, support a redeposition mechanism. Alternative interpretations include (i) diagenetic segregation of silica into chert-rich beds and silica-poor claystones from initially homogeneous siliceous muds, or (ii) variations in surface-water productivity, or/and (iii) variations in the input rate of the terrigenous component. These processes, however, do not adequately explain the sharp lithologic boundaries between the chert and interbedded shale layers which should have been obliterated by the activity of burrowing organisms, if these sediments were deposited through slow pelagic accumulation. Nearly all "bedded cherts" contain shale interbeds, often of red or green color, that comprise 5-40% of the sequence.

In some cases, the chert beds display none of the evidence for redeposition listed above, but still have sharp bottom and top contacts. This is the reason why some investigators prefer variations in biogenic productivity and/or diagenetic segregation as origin for these deposits (*e.g.*, Diersche (1980) for the well-bedded Upper Jurassic radiolarites of the Eastern Alps), although the lack of primary sedimentary structures may be due to other reasons (*i.e.*, diagenetic obliteration during recrystallization and/or uniform small grain size). There seems to be general agreement, however, that the bedding in radiolarian cherts cannot be ascribed to a single process (*e.g.*, Baltuck, 1983; Hein and Karl, 1983; Jenkyns and Winterer, 1982). Recognition of symmetrical geochemical changes (from the centre of beds upward to the top and downward to the base) and symmetrical grading of radiolarian abundance (Mizutani and Shibata, 1983; Sano, 1983; Steinberg *et al.*, 1983) lend new support to the diagenetic origin of some bedded cherts.

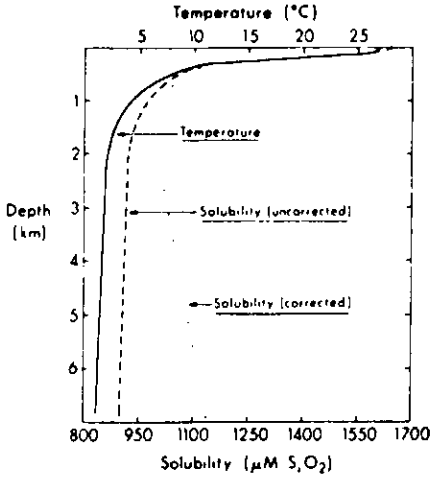

Figure 3 *Solubility of biogenic silica in the Central equatorial Pacific estimated as a function of temperature and pressure (dotted line, from Hurd, 1983, after Griffin, 1980).*

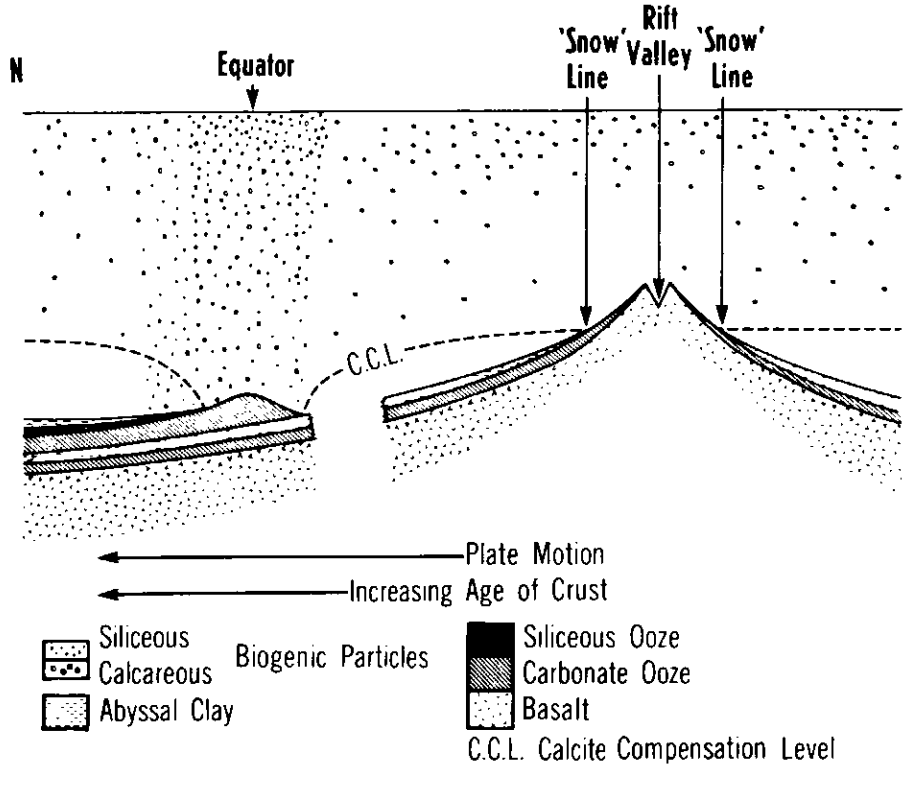

Figure 4 *Pelagic stratigraphy model for the Pacific Ocean showing duplication of the biogenic sediment sequence due to the northwestward passage of the Pacific plate under the equatorial high-productivity belt (from Hesse* et al., *1974). Section oriented approximately NW-SE The calcite compensation level (CCL) acts as a "snow line". The East Pacific Rise and other regions rising above it are covered with light-coloured biogenic oozes, areas below the CCL and outside the belts of siliceous ooze are characterized by red-brown abyssal clay (Figure 2)*

(For recent reviews of radiolarian cherts *see* Jenkyns and Winterer, 1982; Jones and Murchey, 1986).

Shallow water cherts. The effects of upwelling are not restricted to open ocean environments or the continental slope. Upwelling zones may transgress from the slope onto the shelf. Biogenic siliceous sediments, therefore, are not restricted to deep-water pelagic environments, but may onlap the continental shelves and even occur on the inner shelf, as for example, off Namibia (Calvert, 1983). Tertiary opaline claystones of the coastal plains of the southeastern United States are ancient equivalents associated with transgressive-regressive cycles (Weaver and Wise, 1974). The Monterey Formation of California, one of the better-studied ancient chert formations on land, was deposited in a Miocene continental margin environment composed of deeper and shallower water sites (Isaacs *et al.*, 1983) comparable to the present California borderland. The Monterey Formation is one of the principal sources of, as well as an important reservoir for, California's onshore and offshore hydrocarbon accumulations, underlining the economic significance of organic-matter rich biogenic siliceous sediments (Isaacs, 1984).

Biogenic silica accumulations in nearshore environments may occur in close association with shallow-water carbonates and give rise to chert nodules. Shallow-water sandstones and siltstones, on the other hand, are remarkably poor in concretionary silica (Dapples, 1967), in contrast with continental deposits. The Tertiary shallow marine examples of the Atlantic and Gulf coastal plains of the US (mentioned above) contain silica-cemented sandstones that appear to have received the silica from the associated opaline claystones (Wermund and Moiola, 1966; Wise and Weaver, 1973; Weaver and Beck, 1977; Carver, 1980). In Paleozoic sequences, siliceous sponge spicules are often abundant, particularly in deep basinal deposits, but have also been considered as shoreline indicators (Cavaroc and Ferm, 1968; Lane, 1981). In a number of cases, spicules provide an adequate source of silica. Their diagenetic end-products are nodular cherts or chert nodules which often occupy only a small fraction of the total volume of the carbonate or evaporite host rock. These nodular cherts are distinctly different from the ancient bedded cherts in the rock record and the biogenic siliceous oozes, muds and cherts on and under the modern ocean floors. Diagenesis of the latter will be discussed in this paper. The diagenesis of the former may proceed under conditions considerably different from those of the deep-water cherts, and those of the siliceous deposits in alkaline lakes and in soils. The diagenesis of these and other types of chert including silicified wood will be discussed in another paper (Hesse, *in press*), ending with a note on the cherty varieties of Precambrian banded iron formations.

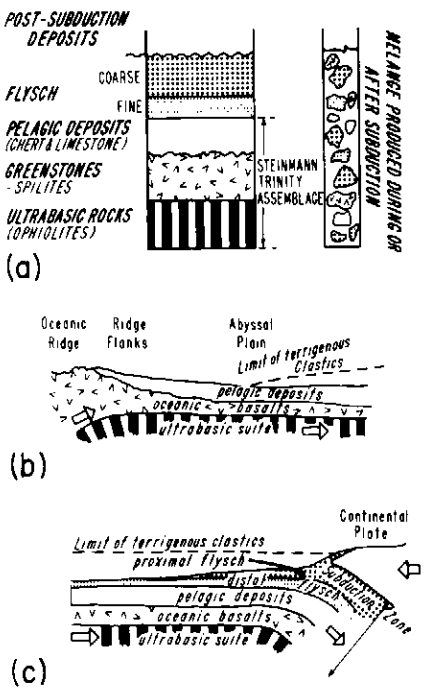

Figure 5 *(a) Schematic representation of the "Steinmann trinity" (= ophiolite stratigraphy) of ultrabasic rocks, altered basalts and pelagic sediments (radiolarian cherts and limestones); (b) origin of the ophiolite stratigraphy through ocean crust generation at mid-oceanic ridges; and (c) its destruction in subduction zones (from Chipping, 1971).*

Stages of Burial Diagenesis in Biogenic Siliceous Sediments

During burial, biogenic siliceous sediments undergo a characteristic sequence of mineralogic transformations which may be subdivided into three stages, each defined by the predominance of one of the common low-temperature silica phases (Calvert, 1971):
(1) the opal-A stage of siliceous oozes or muds;
(2) the opal-CT stage of porcelanites; and
(3) the microquartz or quartz stage of chert *sensu stricto* (quartz chert).

Silica recrystallization in petrified wood follows the same sequence, whereas some cherts in carbonates and some non-biogenic cherts may also follow different diagenetic pathways as discussed in Hesse *(in press)*.

Porcelanite and chert do not simply reflect the mineralogical difference between opal-CT and quartz as a result of progressive diagenesis. As suggested by Isaacs *et al.* (1983), primary compositional differences, such as the ratio of clay minerals to silica minerals, are often more important in determining textural and physical properties on which the distinction of rock types is based. In the Monterey Formation, the most silica-rich sediments (pure diatomites) form rocks that appear macroscopically as cherts although they may still consist entirely of opal-CT. Diatomaceous shale on the other hand, has the appearance of porcelanite, even after having reached the quartz stage.Because these rock names were originally designed for the field description of siliceous rocks (Bramlette, 1946), they will be used in this review in the sense of Isaacs *et al.* (1983). That is, the distinction between porcelanite and chert will be based primarily on detrital content. Often, however, porcelanite consists predominantly of opal-CT, and chert predominantly of (micro-)quartz, this being the reason why Calvert (1971) first suggested a nomenclature of siliceous rocks strictly based on mineralogy, a usage largely followed by the Deep Sea Drilling Project (*e.g.*, Riech and v. Rad, 1979). See however, Pisciotto (1981) for the alternative descriptive approach.

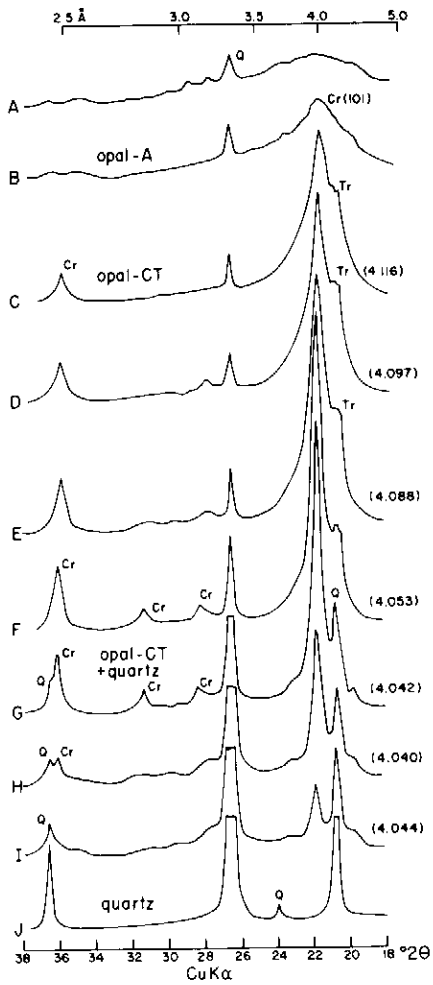

Figure 6 *(A) X-ray diffractogram for opal-A (broad hump at about 4Å) and detrital quartz* **(Q)** *in diatomaceous shale.* ***(B to I)*** *peak-sharpening and shift in position of the (101) diffraction of opal-CT with progressive burial in the Monterey Formation of California. Doublet peaks at 4.1Å and 4.3Å for cristobalite* **(Cr)** *and tridymite* **(Tr)**, *respectively. Numbers in brackets: cristobalite-d(101) of opal-CT in angstroms.* ***(J)*** *Diffractogram of quartz chert. (Modified from Murata and Larson, 1975, fig. 5).*

The characteristics of the different silica phases and the diagenetic transitions from one phase to the other will be described in the following paragraphs. Important questions discussed are: What are the physicochemical mechanisms involved in the transformations? Are the transformations of opal-A to opal-CT and of opal-CT to (micro-)quartz exclusively due to dissolution-reprecipitation reactions as favoured by recent findings, or is there any evidence for the solid state reactions originally suggested by Ernst and Calvert (1969)? What are the rate-controlling factors? In particular, how does lithology influence transformation rates? Why is an intermediate state of metastable opal-CT required in the transition from opal-A to quartz?

Characteristics of the Silica Phases in Biogenic Siliceous Sediments

Opal-A: Physical characteristics, solubility, and polymerization. The tests of siliceous microfossils as well as silica precipitated inorganically under earth surface conditions, as in hot-spring areas or desert soils, consist of an X-ray amorphous substance named opal-A (Jones and Segnit, 1971), because it is mineralogically similar to precious opal. The X-ray pattern of this near-amorphous substance with a broad hump near 4Å (Figure 6a) resembles that of glass. This material is very porous and has a substantial water content (4-9% in precious opal). Opal-A dissolves easily in seawater, which is highly undersaturated with respect to opaline silica everywhere in the modern oceans. Seawater contains from a fraction of a part per million to 10-15 ppm dissolved silicon (or up to 160-250 $\mu M \cdot L^{-1}$), *i.e.*, considerably less than the equilibrium solubility of amorphous silica, which is between 60 and 130 ppm at 25°C and a pH < 9. Silica-secreting marine micro-organisms thus must extract dissolved silicon from seawater at concentrations well below the thermodynamic equilibrium solubility of opal-A, but will raise it to saturation under the catalyzing influence of enzymatic reactions. Concentrations of dissolved silicon in the ocean are lowest in surface seawater because of the extraction by organisms. They increase with water depth because of the dissolution of siliceous tests settling through the water column, leading to a mid-depth maximum. A subsequent decrease at greater depths is caused by the renewal of bottom waters from silicon-poor surface-water sources in polar regions, especially in the North Atlantic. Bottom maxima in dissolved silicon, on the other hand, are associated with belts of siliceous sediments, particularly diatom oozes (Edmond *et al.*, 1979b), with Antarctic Bottom Water, and areas of hydrothermal activity.

In inorganic systems, equilibrium solubility of silica depends on a number of factors besides temperature (Figure 7a), notably surface area and particle size of the solid silica phase (Figure 7b), to a lesser extent pressure as stated in a previous section (Figure 7c). It increases significantly for a pH greater than about 9 (Figure 7d, Williams *et al.*, 1985; Williams and Crerar, 1985). Other ions in solution can have distinct effects on dissolution rates of solid silica. Dissolved Al and Fe which adsorb to the opal-A surface suppress opal-A solubility and dissolution rate (Iler, 1955, 1973; Lewin, 1961). Also, ageing of the biogenic siliceous tests affects solubility through changes in surface area and crystallite size in the shell wall (Hurd and Theyer, 1975). Equilibrium solubilities of the other common low-temperature silica polymorphs, opal-CT and quartz, are respectively one and two orders of magnitude lower than those of opal-A (Figure 7a), although for opal-CT no thermodynamic data exist.

Because of the significance of silica solubilities for the diagenetic transformations of the solid phases, a somewhat closer look at the chemistry and kinetics of the dissolution and precipitation processes, including polymerization, of silica is in order. In solutions of pH < 9, dissolved silicon is present predominantly in the form of undissociated silicic acid H_4SiO_4 (orthosilicic or monomeric silicic acid). The dissolution of solid silica can be written as

$$SiO_2\,(s) + H_2O = H_4SiO_4\,(aq)\ .$$

At equilibrium, the solubility product, K_{sp}, thus approximates the activity $a(H_4SiO_4)$. In solutions of pH > 9, orthosilicic acid dissociates (Figure 7d), in a first step into

$$H_4SiO_4\,(aq) \rightarrow H_3SiO_4^- + H^+,$$

and for higher pH values (> 13) in a second dissociation step into

$$H_3SiO_4^- \rightarrow H_2SiO_4^{2-} + H^+$$

These dissociations raise the solubility significantly, because the total dissolved silicon concentration is the sum of the dissociated and undissociated species.

In supersaturated solutions, dissolved silicon polymerizes forming first oligomers (dimers, tetramers and ring structures), then later higher-molecular-weight polymers as siloxane bonds (Si-O-Si) develop through combination of silanol (-Si-OH) groups:

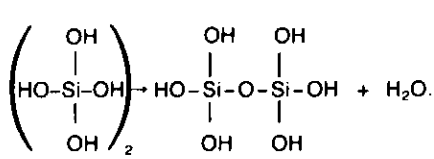

(silanol) (siloxane)

Williams and Crerar (1985) emphasize the fact that low-molecular-weight oligomers also contribute to the total solubility in solutions at or near opal-A saturation, contrary to the assumption in most previous experimental work that all dissolved silicon is monomeric in such solutions. Oligomers may even persist in undersaturated solutions at tem peratures below 130°C, although under such conditions they will gradually depolymerize (*e.g.*, Krauskopf, 1956). At concentrations below opal-CT saturation, monomeric silicic acid is the only form present. On the other hand, if supersaturation persists, high-molecular-weight polymers (with molecular weights up to 10,000) form. Such polymers have colloidal dimensions (greater than 50Å) and may remain suspended as sols as long as pH remains relatively high and salinity low; otherwise they will form cross-links with neighbours and coagulate into gels (Figure 8a).

Silica polymers display a negative surface charge, which results in a point of zero charge (PZC, *i.e.*, the pH at which the residual surface charge disappears) as low as 2 ± 0.5 (Parks, 1965). Silica colloids thus repel each other unless the surface charge is neutralized by other ions in solution such as metal hydroxides. Interestingly, the hydroxide most commonly used for silica precipitation in industrial applications, $Mg(OH)_2$ (Iler, 1979), is also thought to be instrumental in the nucleation of opal-CT, as discussed below.

The ultrastructure of precious opal shows a hexagonal or cubic closest packing of opal-A spheres that are remarkably uniform in size (Iler, 1979). Apparently, they are deposited from colloidal particle suspensions of uniform size that grow in supersaturated solutions in the absence of natural coagulants. The sphere diameter is in the appropriate size range (0.17-0.38 μm) to diffract visible light (in the same manner crystal lattices diffract x-rays) and to produce the iridescent diffraction colours of gem opals. These spheres consist of several concentric shells of primary smaller spheres with diameters ranging from 100 to 500Å depending on the opal type (Figure 8b). Uniform size of the primary spheres apparently is achieved by the dissolution of smaller polymers and redeposition of the dissolved silica on the larger ones (Darragh *et al.*, 1976).

Opal-CT: Ultrastructure. The "CT" in opal-CT stands for cristobalite/tridymite (Jones and Segnit, 1971) and denotes a modification of opal which has structural characteristics of both α-cristobalite and α-tridymite. Opal-CT thus is the low-temperature form (α-form) of cristobalite/tridymite formerly called lussatite (Mallard, 1890). In opal-CT, cristobalite alternates randomly with unidimensionally disordered tridymite layers. On X-ray powder diagrams, the main diffraction peak of opal-CT is a doublet at 4.1 and 4.3Å (Figures 6b to 6i). Wise *et al.* (1972) first observed the occurrence of opal-CT in the form of small spheres less than 5 μm in diameter in deep-sea drilling samples under the scanning electron microscope (SEM). These spheres, which consist of an interpenetrative growth of tiny

cristobalite/tridymite blades, were called opal-CT lepispheres (Figure 9a) by Weaver and Wise (1972). On high-resolution SEM photos, lepispheres in their incipient growth stage show sets of subparallel opal-CT blades which penetrate each other at angles between 70° and 71°. Individual blades are 2-5 μm long and 0.05-0.1 μm thick, and display ragged or rounded edges (Figure 9b). The penetration angle corresponds to the angle of 70°32′ at which equivalent faces of a cristobalite octahedron intersect one another (Figures 9c,d). Flörke *et al.* (1976) give a plausible crystallographic interpretation for the peculiar twinning behavior of opal-CT in the lepispheres, which appears to be dictated by crystal growth kinetics. At more advanced growth stages the skeletons will coalesce to form lepispheres. The diameter of individual lepispheres usually does not exceed the length of the blades (about 5 μm) of which they are composed. Larger lepispheres are almost invariably aggregate forms (Figure 9e; see also Carver, 1980, figs. 1C, 1D, 3A, 3B). Relics of former opal-CT lepispheres in Paleozoic cherts which have been portrayed in the literature (*e.g.*, Jones and Knauth, 1979; Meyers, 1977) are invariably too large for genuine lepispheres, unless they are aggregates.

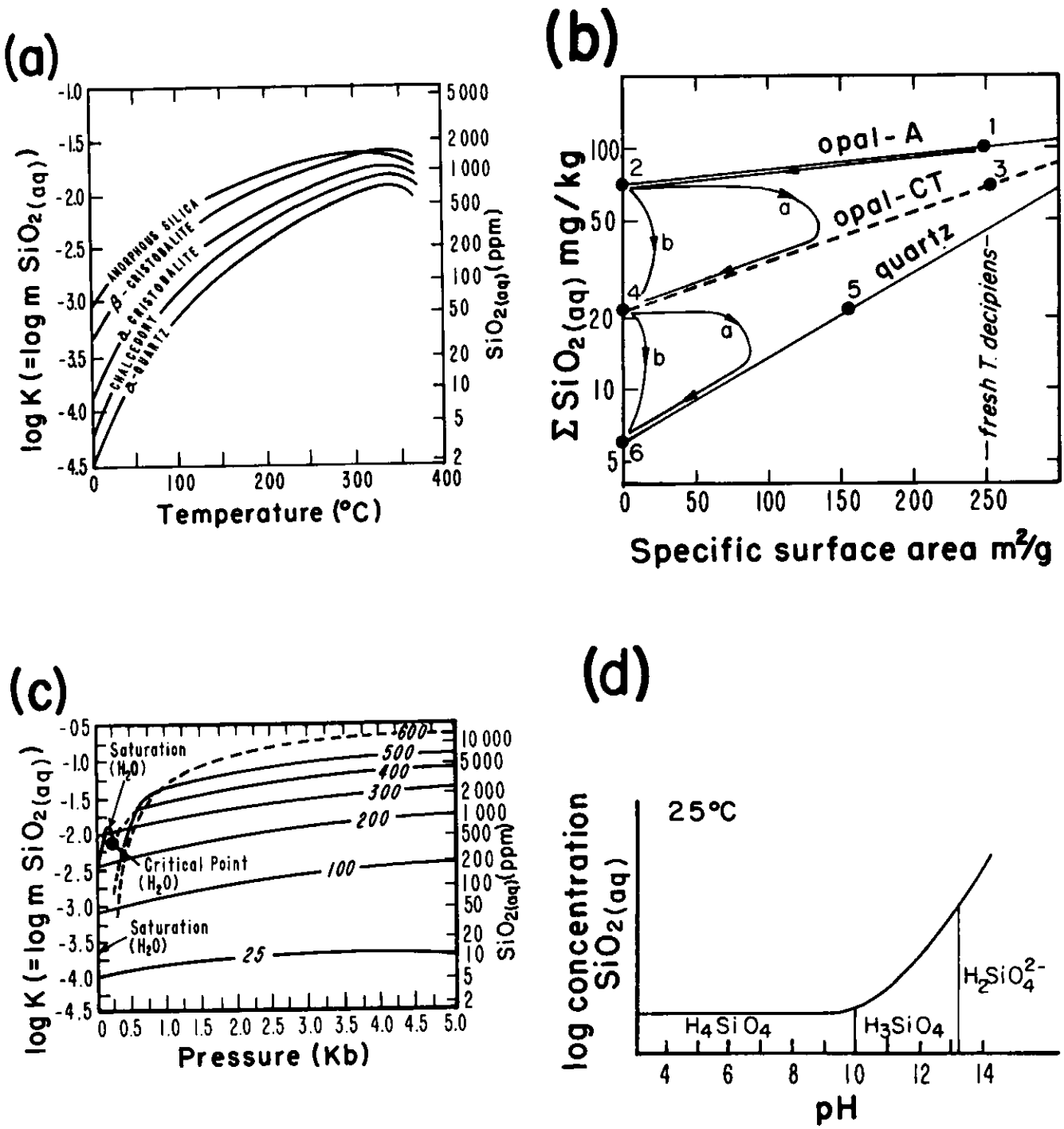

Figure 7 *Solubility diagrams for various silica phases as a function of* **(a)** *temperature (from Williams and Crerar, 1985; modified after Walther and Helgeson, 1977);* **(b)** *specific surface area (from Williams* et al., *1985);* **(c)** *pressure for quartz at various temperatures between 25° and 600°C (from Williams and Crerar, 1985; modified after Walther and Helgeson, 1977); and* **(d)** *pH (from Williams and Crerar, 1985; after Volosov* et al., *1972).*

Low-temperature tridymite and cristobalite as separate, distinct mineralogic phases. The occurrence, under special geologic conditions, of low-temperature tridymite and cristobalite as separate mineralogic phases distinct from opal-CT was proposed by Tada and Iijima (1983). The disordered low-temperature tridymite (α-tridymite) is characterized by a relatively broad diffraction peak at 4.11 Å on X-ray powder diffractograms obtained from mixtures of α-tridymite, α-cristobalite and opal-CT. On the same diffractograms, the better ordered α-cristobalite (also called opal-C) produces a sharper diffraction peak at 4.04 Å. As will be shown later, both the 4.11 and 4.04 Å peaks have also been attributed to opal-CT at various stages of burial maturation (Murata and Larson, 1975). The justification given by Tada and Iijima (1983) for distinguishing a disordered tridymite from 4.11Å-opal-CT is that it did not recrystallize to a 4.04Å-phase upon heating (for 11 days to 1100°C) contrary to what was expected. In nature, this low-temperature tridymite is observed as a pore-filling cement precipitated from ground water or hydrothermal solutions in silicic volcanic rocks . The low-temperature α-cristobalite is also generally associated with volcanic and silicic volcaniclastic rocks. In deep-sea sediments it has been reported from volcanogenic sediments overlying basalt in the West Pacific (Lau Basin, Griffin *et al.*, 1972) and Central Pacific (Zemmels and Cook, 1973).

Nature of the Transformation Mechanisms

Opal-A to opal-CT transformation. Only a small percentage of the large amount of biogenic silica (opal-A) produced by planktonic organisms in the surface ocean reaches the sea floor, and only a fraction of this escapes dissolution during the first metres of burial. Even this very small proportion of solution-resistant species will ultimately undergo dissolution at greater sub-bottom depths. The effects of progressive dissolution have been documented by systematic SEM studies of diatom oozes (*e.g.*, Hein *et al.*, 1978). Breakage of partially dissolved diatom valves accompanies and enhances dissolution, culminating in the complete destruction of the tests. Dissolved silicon profiles from DSDP holes in the pelagic realm reflect the dissolution of solid silica particles in the subsurface. These profiles show consistent increases in dissolved silicon with sub-bottom depth, not uncommonly exceeding 1 mM (or 60 ppm) at a few 100 m below the sea floor. Concentrations may fluctuate considerably with depth, but these fluctuations are generally superimposed on an overall trend of downward increasing silica concentrations (Figure 10). In many holes, however, the gradual downward increase is followed by an abrupt decrease below a certain depth (*e.g.*, DSDP site 495, Harrison *et al.*, 1982; site 570, Hesse *et al.*, 1985) consistent with reprecipitation as opal-CT. In the examples mentioned, this is substantiated by the recovery of the first porcelanite nodules from this depth. Below this depth, a second less pronounced maximum may be observed in holes with sufficient penetration, probably corresponding to the dissolution of opal-CT and the subsequent reprecipitation as quartz described in the next section.

Continued dissolution of opal-A in the sediment during burial is the result of slowly increasing temperature and pressure. Siliceous tests of diatoms and Radiolaria have large specific surface areas ranging from several tens to 450 $m^2 \cdot g^{-1}$ (Kastner *et al.*, 1977), compared with 0.1 $m^2 \cdot g^{-1}$ of crushed quartz in the size range of 3-5ϕ (25-75μm) (Van Lier *et al.*, 1960). The sieve structure of the porous test walls of these organisms (Figure 9f) is only partly responsible for these large specific surface areas. As Hurd *et al.* (1979) have shown, it is ultimately the size of the small opal-A domains (2.5-4.5Å diameter) in the tests which causes the high specific surface areas. Surface area can significantly affect solubility. When the surface area to volume ratio of a substance becomes large, small changes in pressure and temperature may then markedly influence its solubility. Suppression of solution inhibiting factors such as the removal of protective coatings of organic matter may further increase solubility. This explains the continuation of opal-A dissolution during burial, even though up to 99% of the opal originally produced may have already been dissolved during settling and initial burial.

Dissolution during sediment burial, in contrast with the earlier dissolution, occurs in a more or less closed system in which concentration levels may reach supersaturation before opal-A dissolution has gone to completion. In this case, dissolution will be interrupted by reprecipitation of a less soluble non-biogenic opal-A which forms overgrowths on partially dissolved siliceous tests. These inorganically precipitated overgrowths are called opal-A′ (Hein *et al.*, 1978).

Figure 9 ***(opposite page)*** ***(a)*** *Small opal-CT lepispheres (2-3 μm in diameter) growing on euhedral calcite crystals in a cavity in partially silicified Maestrichtian chalk, DSDP 14-144-3-2, 103-104 cm.* ***(b)*** *Opal-CT blades of a "juvenile" lepisphere displaying twinning angle of 70° corresponding to the intersection angle of the faces of a cristobalite octahedron as shown in* ***(c)*** *and* ***(d)*** *(from v. Rad* et al., *1977).* ***(e)*** *Composite lepisphere 50 microns in diameter which resulted from coalescence of numerous individual lepispheres, DSDP 12-117A-2cc (from Flörke* et al., *1976).* ***(f)*** *Sieve structure of diatom frustule. (SEM photos in Figures 9a, b, e, f: courtesy U. v. Rad).*

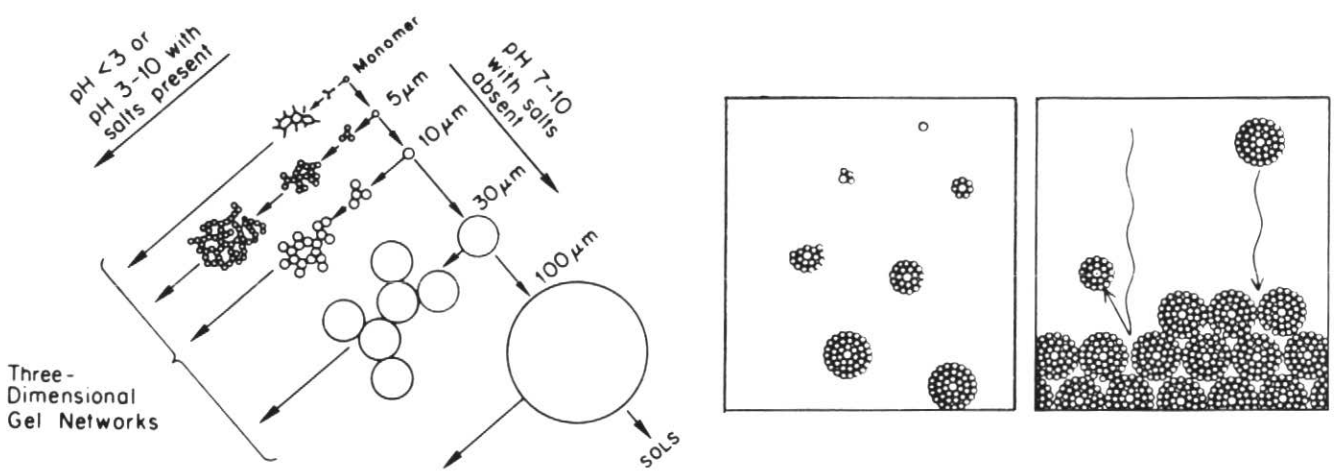

Figure 8 ***(a)*** *Polymerization behaviour of dissolved silicon as a function of pH and ionic strength of the solution (from Williams and Crerar, 1985).* ***(b)*** *Formation of precious opal by deposition of large spheres of opal-A of uniform size in a hexagonally or cubically closest packed layer. Large spheres consist of concentric shells of smaller primary spheres (from Williams and Crerar, 1985; after Darragh* et al., *1976).*

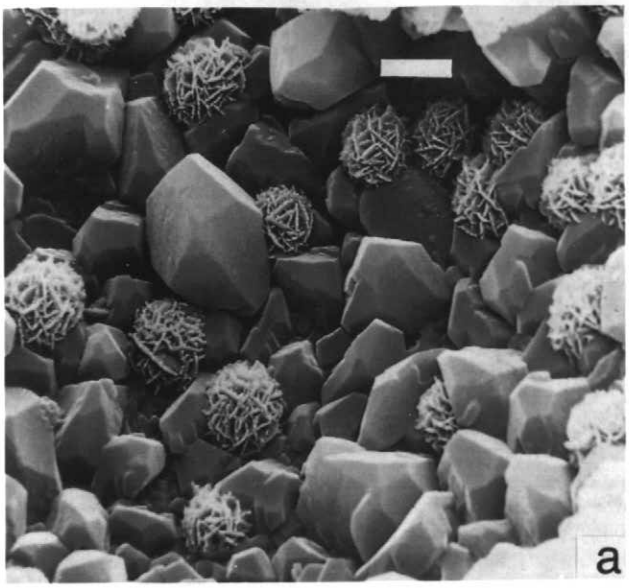
a

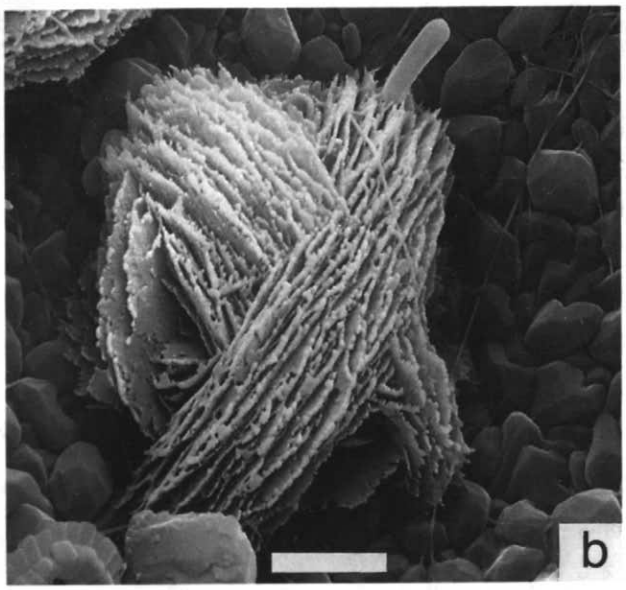
b

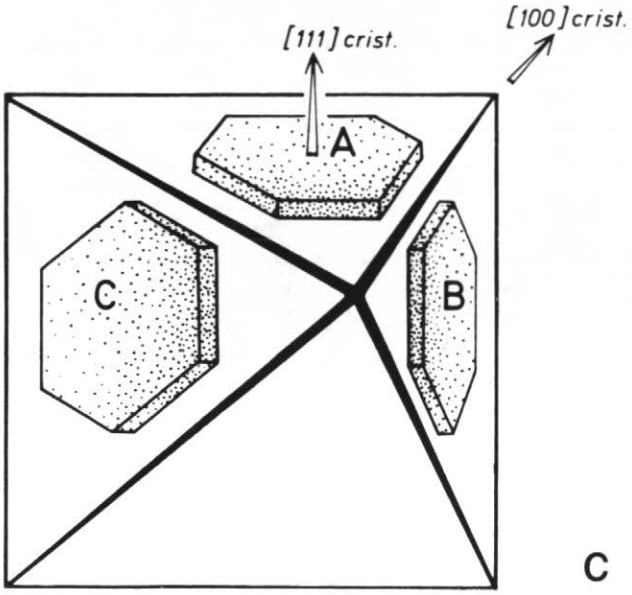
[111] crist.
[100] crist.
A
B
C
c

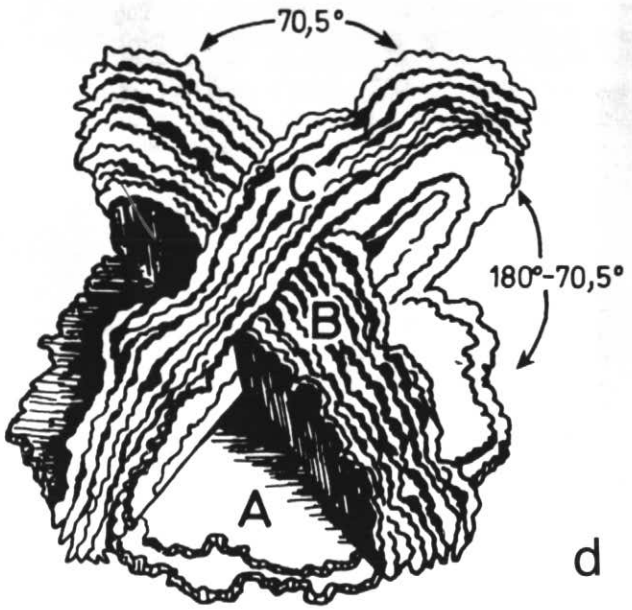
70,5°
180°-70,5°
A
B
C
d

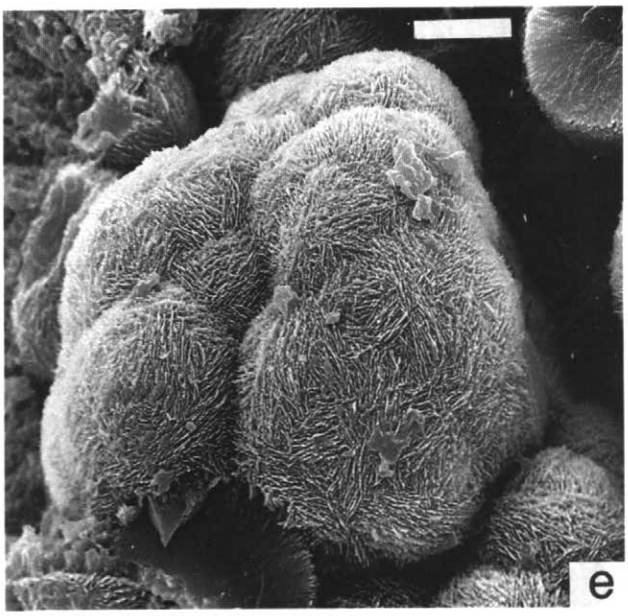
e

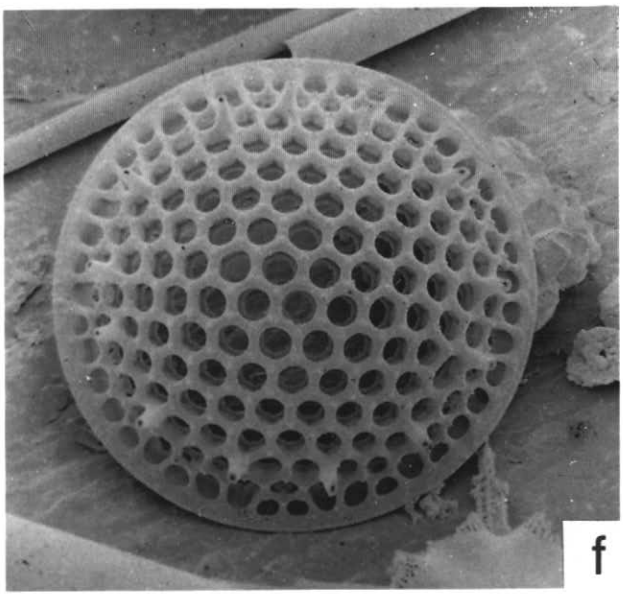
f

Crystallite size calculated from X-ray diffraction data for opal-A' is larger (20-27Å) than for biogenic opal-A (12-16Å). In individual DSDP holes, opal-A' overgrowths have been found to occur only over a narrow stratigraphic range of a few metres, indicating that they redissolve shortly after formation together with the remaining opal-A (Hein *et al.*, 1978). Therefore they are rarely observed. Their presence, however, may explain some of the fluctuations seen in the concentration – depth profiles of dissolved silica (Figure 10).

Recognition of inorganically precipitated opal-A' by Heath (1969) and Hein *et al.* (1978) demonstrates that the opal-A to opal-CT transformation is not a single-step process but involves a series of dissolution–reprecipitation reactions as postulated theoretically by the model of Williams *et al.* (1985). This model is based on surface-area effects (Figure 7b). The hypothetical SiO_2-H_2O system used is a closed system at constant temperature, pressure, pH and consists of the pure reactants. In this system, opal-A of a diatom species with a specific surface area, say of 250 $m^2 \cdot g^{-1}$ (*i.e.*, *Thalassiosira decipiens*, Figure 7b), will have a solubility of about 100 ppm. If dissolution of the frustules of this species is fast relative to nucleation and growth of other new silica phases, then the solution will soon become supersaturated with respect to opal-A of a lower surface area (*i.e.*, opal-A'). The solution is also supersaturated with respect to opal-CT of any given surface area to the left of point 3 in the diagram, as well as with respect to any quartz. The nucleation and growth rates of opal-CT will be slower than those of any opal-A, and those of quartz will be slower than those of opal-CT, because opal-CT and quartz are more highly ordered forms of solid silica compared to opal-A. Under these assumptions, an opal-A' with a surface area lower than that of opal-A will precipitate and the solution will evolve along the pathway from points 1 to 2 shown in Figure 7b – a process called "Ostwald ripening" (Iler, 1979; Williams *et al.*, 1985). Near point 2, the effect of surface area on opal-A solubility becomes negligible. At this point, the solid silica phase with the next lower solubility, *i.e.*, opal-CT may appear. Opal-CT is preferentially precipitated over quartz, because of its higher nucleation and growth rates. Depending on the dissolution rate of opal-A relative to the nucleation and growth rate of opal-CT, further evolution of the solution will follow pathways from points 2 to 4 either along curve "a" (fast nucleation rate) or curve "b" (slow nucleation rate). In the first case, rapid nucleation (relative to growth) leads to relatively large specific surface area, because the nuclei are small and numerous. Only when the silica removal rate exceeds the dissolution rate of the remaining opal-A, will silica concentration drop off and the surface area of the newly formed opal-CT decrease (curve 2-4a). If, on the other hand, the growth rate of opal-CT exceeds the nucleation rate early in the process, then the fluid should evolve along pathway 2-4b. Analogous considerations should apply to the opal-CT to quartz transformation discussed in a subsequent section, although the structural reorganization within the opal-CT, which precedes this transformation, is interpreted as a solid-state reaction by some authors.

The discovery of the opal-CT lepispheres with the euhedral crystal shapes of the cristobalite/tridymite blades by Wise *et al.* (1972), Weaver and Wise (1972) and Berger and v. Rad (1972) provided the first proof that

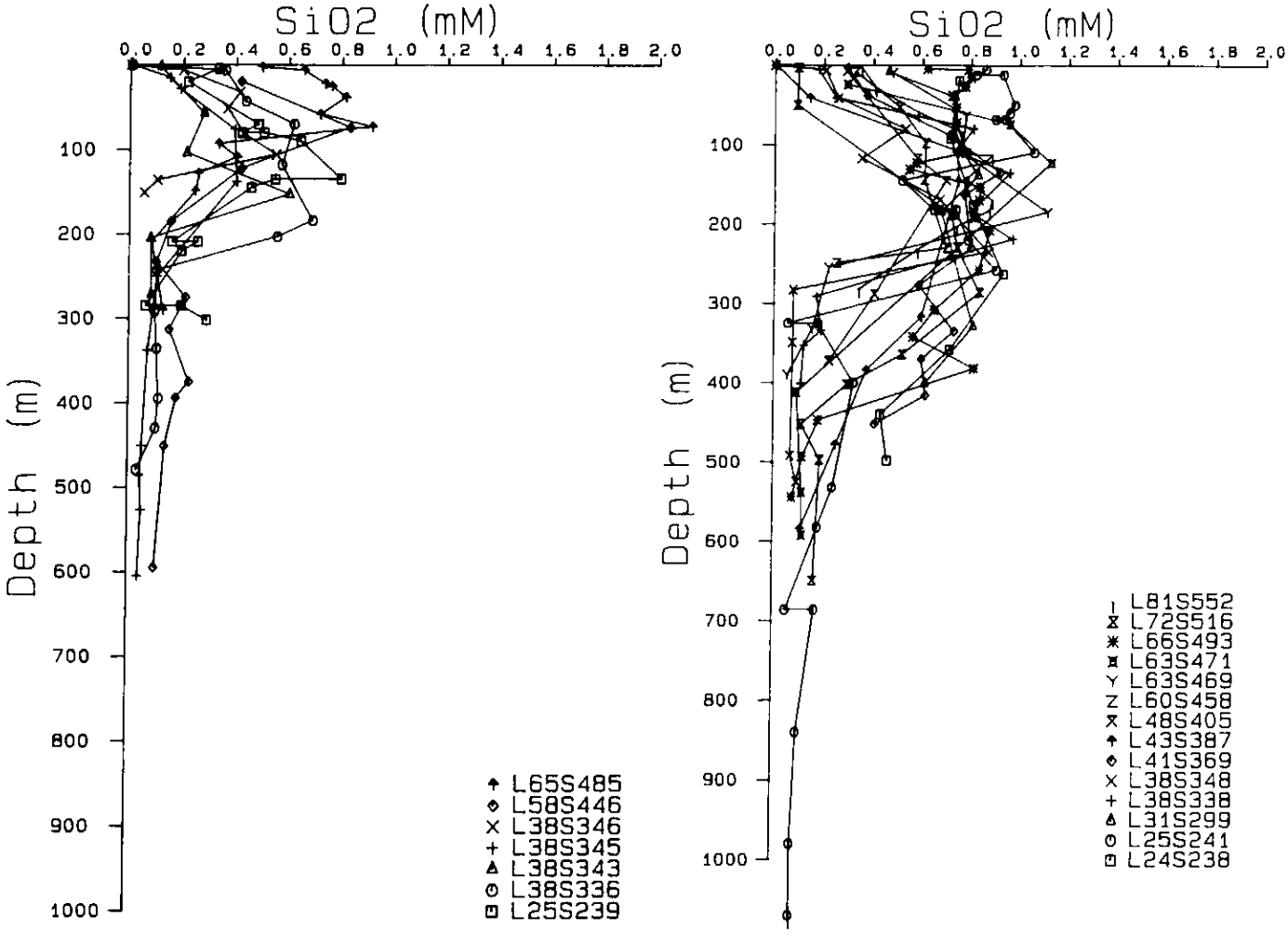

Figure 10 *Concentration of dissolved silicon in pore-water profiles of DSDP holes (L, DSDP leg; S, DSDP site).*

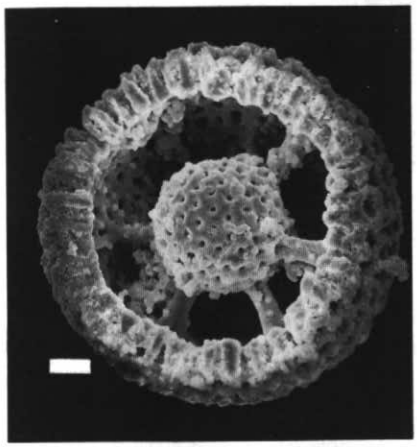

Figure 11 *Radiolarian test replaced by opal-CT, DSDP 41-366-23-1, 42-44 cm (From Riech and v. Rad, 1979. SEM photo, courtesy U. v. Rad).*

the recrystallization of siliceous oozes to porcelanite occurs through a dissolution–reprecipitation mechanism. Lepispheres develop only where crystallization takes place in open pore spaces such as the cavities of microfossils. More commonly, a densely felted mass of opal-CT forms which may impregnate the sediment and/or replace other mineral phases. The latter process may involve pseudomorphic replacement of opal-A by opal-CT in radiolarian tests which perfectly preserves the shape of the shell (Figure 11). The process is still a dissolution–reprecipitation mechanism, which probably proceeds on a grain-by-grain basis with local precipitation immediately following dissolution. Presence of a matrix of organic matter, which is not or only partially affected by dissolution, may serve as a template which helps preserve the original shape of the shell. The process may be similar to the silicification mechanism in ooids (Hesse, 1987) or to the petrification of wood. Where Radiolaria occur embedded in lutitic pelagic limestone, an opal-CT replaced test may simply represent a cast of the former opal-A shell. Conservation of the original shape during the replacement process cannot be used as evidence for a solid-state reaction in the opal-A to opal-CT transformation.

Opal-CT to quartz transformation. The opal-CT to quartz transformation was assumed to be a solid-state mechanism by Ernst and Calvert (1969) and Heath and Moberly (1971), but morphological evidence from scanning electron microscopy (Stein and Kirkpatrick, 1976) makes it more likely that this step is also a dissolution – reprecipitation reaction like the opal-A to opal-CT transformation. In their hydrothermal experiments, Ernst and Calvert (1969) heated opal-CT in distilled water to temperatures of 300°, 400°, and 500°C under 2 kbar pressure. Quartz formed in each experiment. At 500°C the conversion was complete after 30 hours, at 400°C after 300 hours (12.5 days), and at 300°C after 5,000 hours (7 months). For a given temperature the conversion rate seemed to be constant. The concentration of the reactant opal-CT had decreased during the experiment in a more or less linear fashion with time. On the basis of general reaction-rate laws, Ernst and Calvert concluded that the reaction was of zero order with respect to the number of participating reactants; it had to be a solid-state reaction.

Stein and Kirkpatrick (1976) re-examined the reaction products of these experiments under the SEM and found fibrous and euhedral prismatic quartz crystals among the reacted material clearly requiring a dissolved phase for crystallization. After re-evaluation of the experimental data (fraction of opal-CT transformed *versus* time) in the light of nucleation and growth theory (Christian, 1965; Nielsen, 1964), these authors concluded that a sigmoidal curve with slower reaction rates at the beginning and at the end of the conversion process would approximate the rate data better than the straight-line plots of Ernst and Calvert (1969).

Crystallographic structural changes of opal-CT and quartz in the porcelanite and quartz-chert stages.

Sharpening and shift of the opal-CT (101) reflection. The important finding of a dissolution – precipitation step in the opal-CT to quartz conversion by Stein and Kirkpatrick in 1976 did not close the discussion about the nature of the transformation mechanism involved in this phase change. A year before, in 1975, Murata and Larson's results of a high-precision X-ray diffraction study gave rise to new speculations about the possibility of low-temperature diagenetic solid-state reactions. This study revealed characteristic changes in the main diffraction peak of opal-CT (4.1Å) with progressive burial diagenesis. In contrast to Tada and Iijima (1983), this peak is usually attributed to the (101) diffraction of α-cristobalite. In siliceous rocks of the Monterey Formation in the Temblor Range of California, a distinct shift of this peak from 4.11 to 4.04Å is observed with

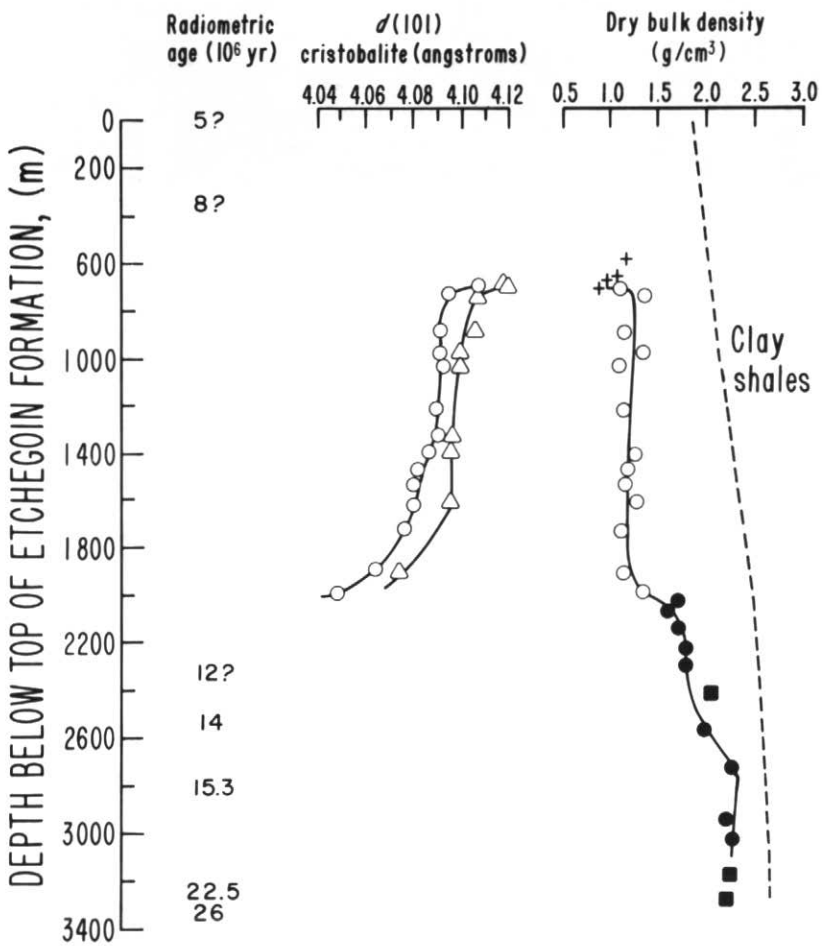

Figure 12 *d(101) spacing of opal-CT in porcelanite (circles) and cherts (triangles) from the Monterey Formation in Chico Martinez Creek, plotted against depth below the top of the Etchegoin Formation (from Murata and Larson, 1975, fig. 6). Density data:* crosses, *diatomaceous shale;* open circles, *opal-CT porcelanite;* half-filled circles, *porcelanite with quartz;* filled circles, *quartz chert;* filled squares, *shale;* dashed line, *densities of normally compacting shales.*

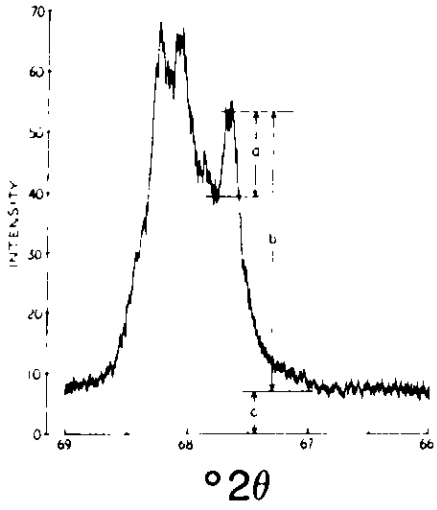

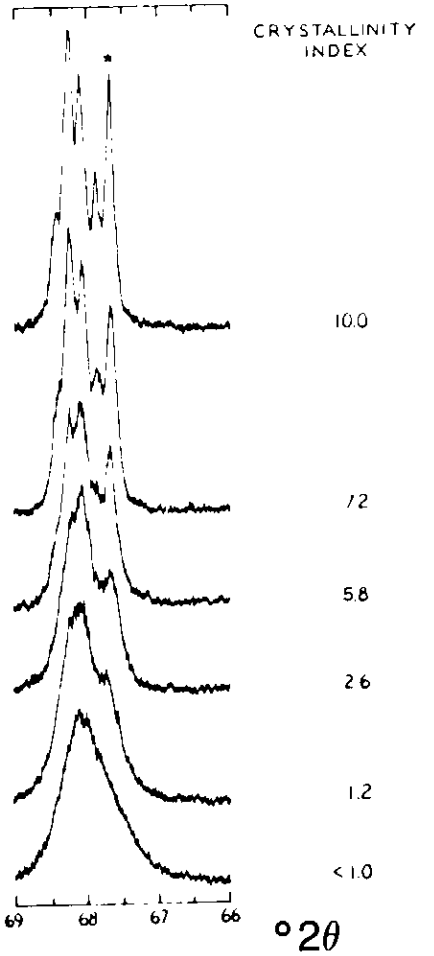

Figure 13 *(a) X-ray diffractogram showing the quartz quintuplet at about 68°2θ, and the parameters* **a** *and* **b** *used to define the quartz crystallinity index* **CI** *of Murata and Norman (1976, fig. 2; for explanation see text).*
(b) Tracings of diffractograms showing increasing quartz crystallinity from bottom to top. Asterisk marks (212) peak at 67.74°2θ which is used for the determination of the index. CuK$_\alpha$ radiation (from Murata and Norman, 1976, fig. 1).

increasing burial (Figure 6). (Slow scanning at a rate of 0.5°2θ·min^{-1} permitted measurement of the peak position with a precision of ±0.0052Å). This decrease in the d-spacing is accompanied by a progressive sharpening of the same peak, a gradual disappearance of the α-tridymite (0001) peak (at 4.32-4.26Å), which is replaced by the quartz (100) peak (at the opal-CT to quartz transition). Minor secondary cristobalite peaks at 3.1 and 2.8Å also appear with increasing burial approximately in the middle of the opal-CT stage. While the shift in the d-spacing of the (101) peak is relatively rapid at the top and bottom of the opal-CT zone in the Temblor Range, it nevertheless proceeds continuously over the entire burial range of the opal-CT zone, albeit very slowly in the middle stages (Figure 12). In contrast, in the Santa Maria Valley, Pisciotto (1981) found the shift to become more rapid with increasing burial depth starting in the middle of the opal-CT zone. The bulk density of the sediments, on the other hand, does not show any systematic increase over this range of burial depths (730-2,030 m below reference level). It stays more or less constant at an average value of 1.16 g·cm^{-3}, but increases abruptly to 1.6 g·cm^{-3} over an 80 m thick sediment interval in the opal-CT to quartz transition zone (Figure 12). Oxygen isotope data from the same burial depths display a similar kind of behavior: no systematic change within the opal-CT zone (average value of $\delta^{18}O$ = +29.4‰ relative to SMOW), but a significant decrease by about 5‰ within a short distance below the porcelanite/chert boundary. Murata *et al.* (1977) concluded from these observations "that the structural ordering of cristobalite, manifested in changes of the d(101) spacing, occurred through reactions in the solid state" within the opal-CT stage, but involved complete dissolution – reprecipitation at the stage boundary with the quartz zone.

As Isaacs *et al.* (1983) pointed out, however, "neither the structure of the mineral opal-CT nor the mineralogic significance of the d-spacing of opal-CT are" sufficiently well understood to interpret the changes in the structure of opal-CT as an ordering process in the strict sense, although this is what most authors assume. For instance, the sharpening of the (101)-cristobalite peak with increasing burial may reflect growing crystallite size of the opal-CT which in turn may

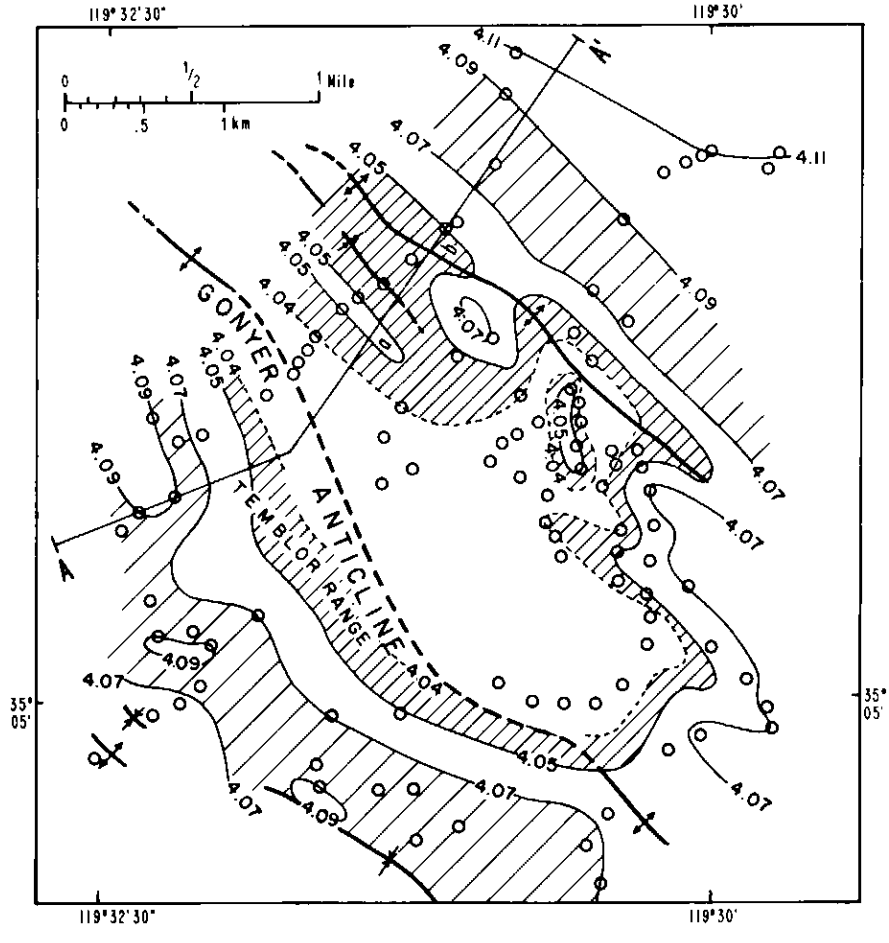

Figure 14 *d(101) spacing isopleths for opal-CT porcelanite in the Temblor Range southwest of Taft (California). These provide an example of "isograd" mapping in low- to intermediate-grade diagenetic rocks. Note apparent congruency between structural features and diagenetic trends. (Redrafted after Murata and Randall, 1975, fig. 4).*

result from gradual dissolution of smaller crystals and redeposition of the dissolved silicon on larger ones (– an Ostwald ripening process). This may be considered a reordering process in a general but not in a strict sense. High-precision X-ray diffractograms are sensitive enough to depict such minute structural changes, whatever their physical cause, and therefore record these modifications continuously with burial, whereas standard oxygen mass spectrometry or pycnometry methods may not pick up small but continuous changes with progressive burial. Williams and Crerar (1985) and Williams *et al.* (1985) suggest that some of the seemingly abrupt mineralogical or geochemical changes at the boundaries of the opal-CT stage may in fact be more gradual than they appear to be. Before reaching a certain threshold level characteristic of a diagenetic stage boundary, some of these changes occur so slowly that the less sensitive methods do not see them. Effects will only be seen after a significant portion of the rock has undergone transformation. Alternatively, the oxygen-isotope composition may in fact change very little within the opal-CT stage because the isotopic ratio of growing larger crystals may be inherited from dissolving smaller ones. Density may also change very little because the morphology of the opal-CT blades remains essentially unchanged. These considerations would make the problem amenable to interpretations entirely based on dissolution – reprecipitation reactions and would eliminate the need for solid-state reactions, which at the low temperatures of diagenesis are prohibitively slow.

The relationship between specific surface area and solubility schematically shown in Figure 7b also explains why opal-CT is required as an intermediate metastable phase in the sequence of diagenetic silica transformations. Quartz cannot form directly from the dissolution of opal-A, at least not from an equilibrium solution, because silicon solubility in equilibrium with opal-A of any specific surface area is too high. At such high silicon concentrations the faces of any embryonic quartz crystal would be crowded by silanol groups which would not have time to be properly fitted into the crystal lattice. Quartz growth will be blocked and a less "well-ordered" phase, opal-CT, will form instead. Only when the "equilibrium solubility" of this phase (for which no precise thermodynamic data exist) has been lowered sufficiently through Ostwald ripening, will quartz crystallization become possible. Opal-CT is a classical example for Ostwald's step rule which states that the transformation of an unstable to a stable mineral phase (at earth surface conditions) often requires one or more intermediate metastable phases. This is an immediate consequence of the crystallization kinetics (Morse, 1988) and answers one of the questions raised at the beginning. However, under special circumstances (see section on reaction rates), it is possible that quartz may precipitate from solutions whose silicon was derived directly from opal-A dissolution but had not reached opal-A equilibrium concentration, or even (the lower) opal-CT concentration.

Crystallinity index of quartz. Sharpening of the (101) cristobalite peak with increasing maturation may be likened to the improvement in quartz crystallinity with progressive diagenesis described by Murata and Norman (1976). The quartz crystallinity index of these authors is based on high-precision XRD measurements at slow scanning speeds (0.25°2θ·min^{-1}) of the high-angle region between 67 and 69°2θ (Cu K_α radiation). In this 2θ range, moderately to well-crystallized quartz produces a quintuplet of XRD peaks of which the (212) peak at 67.74° measures the effects of the recrystallization of cryptocrystalline to microcrystalline authigenic quartz during diagenesis and low-grade metamorphism. The quartz crystallinity index most probably is a measure of crystal size and is defined as

$$CI = 10Fa/b$$

where *a* is peak height on the high-angle side, *b* is the total peak height (as shown in Figure 13a) and *F* is a scaling factor which varies with instrumental settings and adjusts the crystallinity index to a scale of 0 to 10. The crystallinity of authigenic quartz (e.g., in the Monterey Formation) is characteristically poor (2.0 to 3.2), even in quartz cherts *sensu stricto*. Cretaceous quartz cherts in the West Pacific at about 400 m sub-surface depth have crystallinities generally less than 1 (using a scaling factor of 1.36, Pisciotto, 1980). Franciscan cherts show considerably better crystallinities (Figure 13b), but reach high values (above 8.0) only in metamorphosed rocks (Murata and Norman, 1976).

Opal-CT d(101) spacing and quartz crystallinity as mapping tools for diagenetic grade. Variations in the d(101) parameter of opal-CT have been used to map regional maturation levels in relatively low-grade diagenetic rocks (Murata and Randall, 1975)

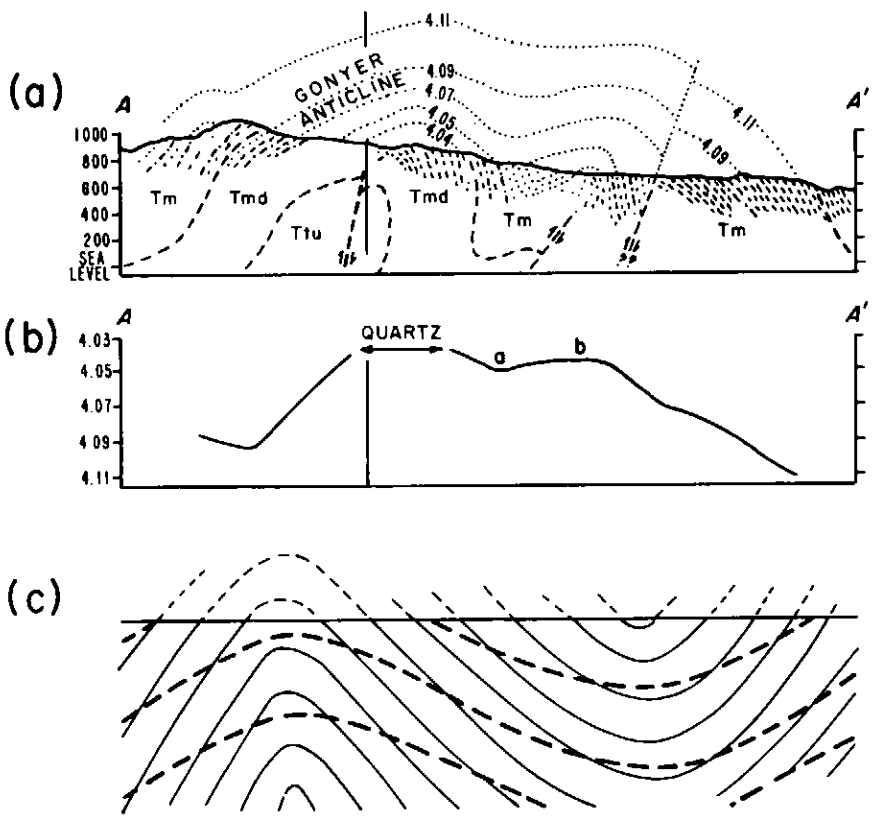

Figure 15 *(a) Geologic cross-section with reconstructed d(101) spacing profiles for opal-CT in the Temblor Range showing near-concordant relationship between folding and maturation levels. For location of section A-A' see Figure 14. (Redrafted after Murata and Randall, 1975, fig. 5B).*
(b) d(101) spacings of opal-CT in surface samples along line A-A'. Region marked "quartz" indicates replacement of porcelanite (opal-CT) by quartz-chert, where d(101) dropped below the lower limit of 4.04 Å for opal-CT. (From Murata and Randall, 1975, fig. 5C). Vertical line: bend in profile.
(c) Schematic representation of discordant structural and maturation patterns (from Mizutani, 1977). Dashed lines, d(101) isopleths; continuous lines, bedding. Note that the reconstructed d(101) isolines in **(a)** *dip less steeply than the geologic structures, suggesting that opal-CT maturation was still in progress when tectonic deformation started. Alternatively delayed crystallographic changes might indicate lithologic control.*

comparable to isograde mapping in higher-grade metamorphic terrains. The contour-lines of iso-d-spacings in the Monterey Formation of the Temblor Range of California generally conform to the geological structures (Figure 14). The lowest d-spacings (4.05 to 4.04 Å) straddle the axes of anticlines. However, as Mizutani (1977) noticed, the dip of the reconstructed iso-d-spacings in the cross-sections of Figure 15 is less than the structural dip. This probably indicates that structural deformation in the Temblor Range started when opal-CT maturation was still in progress (Figure 15c). Alternatively, as discussed below, discordant maturation levels with respect to tectonic structures could reflect lithological effects of the host rocks (Isaacs, 1982).

Keller *et al.* (1985) used quartz crystallinity based on mean apparent crystal size measured under the SEM to map diagenetic and metamorphic grade in the Ouachita Mountains of Arkansas and Oklahoma and in a contact metamorphic aureole on the Isle of Skye, Scotland. Crystal size ranges from less than 1 μm for cryptocrystalline, anhedral quartz in non-metamorphic terrains to more than 100 μm for polygonal, triple-point euhedral quartz in tremolite, diopside and forsterite-grade rocks. The contour maps outline the regional structural trends and depict areas of subsurface igneous activity.

Rate Controlling Factors of the Diagenetic Silica Transformations

Rates of the opal-A to opal-CT transformation in deep-sea environments: Temperature and time. Temperature is the dominant rate-determining factor for the diagenetic silica transformations as illustrated by the experiments of Ernst and Calvert (1969) for the opal-CT to quartz transformation (described above), or the experiments by Kastner *et al.* (1977) for the opal-A to opal-CT transformation (described below). The theoretical basis for this is the Arrhenius equation for the rate constant k of a chemical reaction

$$k = A^{(-E_a/RT)}$$

where E_a is the activation energy, T is temperature, R is gas constant, and A is a frequency factor. During the diagenesis of deep-sea pelagic sediments or silica-bearing shallow-water sediments, pressure effects are generally negligible compared with temperature or other effects. Pressure is generally hydrostatic in these environments and varies only to a small extent over the burial intervals of a few hundred metres in which the first silica transformations take place.

What are the actual *in-situ* temperatures at which the opal-A conversion to opal-CT takes place? Downhole temperature measurements at DSDP sites 184 and 185 (leg 19) in the Bering Sea give temperatures of 35°-51°C at 500-600 m sub-bottom depths in the diatomaceous sediments where the bulk change occurs from opal-A to opal-CT (Hein *et al.*, 1978). In the Temblor Range of California, Murata *et al.* (1977) obtained oxygen isotopic temperatures for opal-CT from porcelanites of the Monterey Formation in the range of 41° to 56°C (mean 48°C) using the fractionation factors of Clayton *et al.* (1972) and Labeyrie (1974) and assuming a $\delta^{18}O$ of 0‰ (SMOW) for the pore water from which the opal-CT precipitated. At a nearby locality, an interstitial water $\delta^{18}O$ of +3.7‰ had to be assumed to obtain the same range of temperatures. These estimates correspond well with a temperature of 50°C calculated on the basis of geothermal gradients by the same authors for an assumed subsurface depth of 700 m in the marine section of the Temblor Range where the transformation to opal-CT allegedly took place. A considerably lower range of temperatures from 9°-27°C was estimated by Pisciotto (1981). This range applies strictly to the top of the opal-CT zone (defined as the depth where opal-CT exceeds 5 weight percent (wt.%)) in the Monterey Formation in drill holes of the Santa Maria Valley in California and is an absolute minimum range. It is based on detailed considerations of the thermal and subsidence history of the region. Opal-CT formation started about 2 million years (m.y.) after deposition and reached a peak after 4 to 10 m.y. (the shorter time corresponding to higher heat flow).

In the pelagic realm away from the mid-ocean ridges, the transformation occurs at shallow sub-surface depths of a few hundred metres where temperature rarely exceeds 20°-30°C. At these low temperatures, the transformations are very slow and the opal-A to opal-CT conversion takes some 10 m.y. to go to completion, and perhaps up to 30 or 50 m.y. for temperatures well below 30°C (Figure 16). The transformation can be traced regionally on seismic reflection profiles because it is associated with the transition from siliceous ooze to porcelanite, which is a major regional lithification event. In the Northwest Pacific, for example, this event is marked by the occurrence of an "opaque" seismic reflector in the subsurface, which first appears at the meridian of Hawaii (at approximately 155°W, Figure 17) in mid-Tertiary siliceous sediments (15-20 m.y. old) which rest on Upper Cretaceous oceanic crust (about 90 m.y. old). This reflector increases in thickness westward from less than 20 m to 200-300 m in the West Pacific where it represents the combined thickness of both siliceous rocks and pelagic limestones as numerous drill holes have shown (*e.g.*, DSDP legs 7, 16, 17, 20, 32, 55, 61, 62, 89). The "opaque layer" can be deciphered on seismic profiles as a distinct interval because it is underlain by older, less brittle and relatively poorly consolidated clayey sediments which produce a "lower seis-

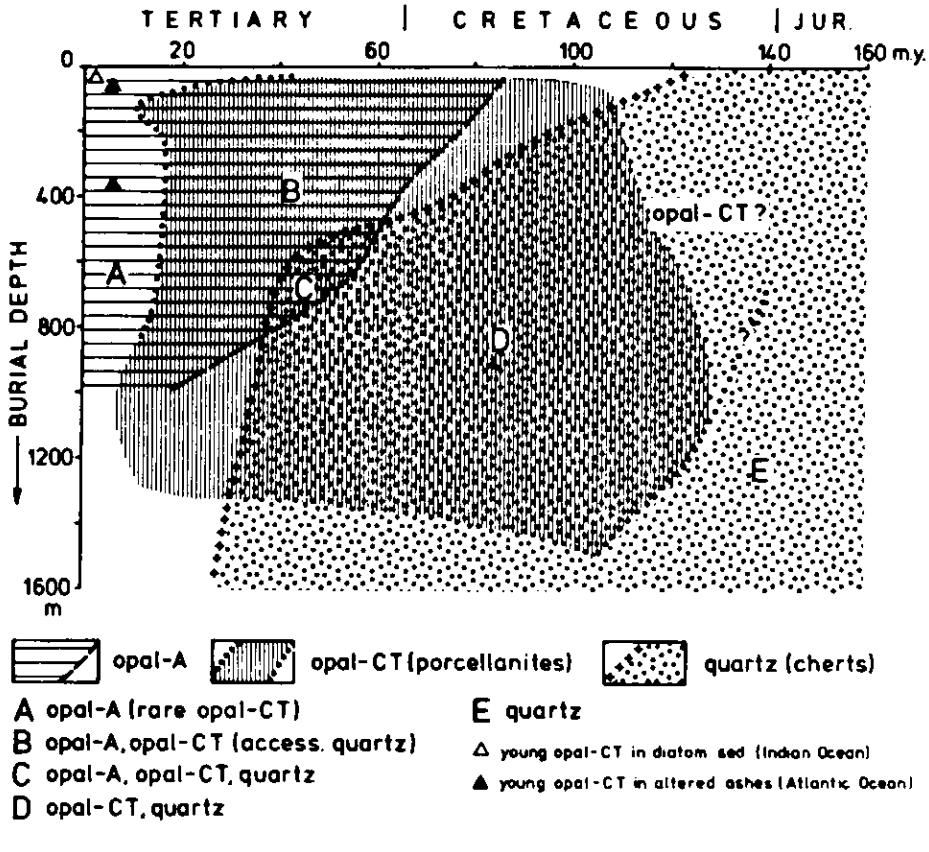

Figure 16 *Age/burial fields for occurrences of opal-A, opal-CT and authigenic quartz in drill-holes of the Deep Sea Drilling Project (from v. Rad, 1979; after Riech and v. Rad, 1979).*

mically transparent layer" in the region. The latter sediments correspond to the lower horizon of brown abyssal clay(-stone) that formed when that part of the Pacific plate which is now north of the equator was still located south of the equator and had first subsided below the CCL (see section on pelagic stratigraphy model, p. 172). The "upper opaque layer" on North Pacific seismic profiles west of Hawaii thus records a diagenetic history that needed an activation time of at least 15 m.y. before it produced bulk physical changes. This illustrates the importance of the factor time which may play the major role in diagenesis, if temperatures are low.

Host-rock lithology as rate-controlling factor. In addition to temperature and time, there are other factors which may promote or retard the diagenesis of siliceous sediments. Since Bramlette's (1946) classical work on the Monterey Formation numerous exceptions from the general maturation sequence "siliceous ooze → porcelanite → quartz chert" have been recognized. For example, in the Monterey Formation, porcelanite and/or quartz chert beds occur within the zone of non-recrystallized diatomaceous mudstone and diatomite, and chert layers occur within the porcelanite zone. Apparently, the diagenetic reactions leading to the silica transformations proceed faster in certain horizons than in adjacent ones. In other cases, the transition to quartz seemed to have occurred directly from opal-A without an intermediate opal-CT stage (*e.g.*, Lancelot, 1973).

As observed during early legs of the DSDP (*e.g.*, v. Rad and Rösch, 1972; Lancelot, 1973; Keene, 1975), lithology of the host rocks has a distinct influence on silica transformations. For example, in clayey sediment sections, silica maturation had reached the opal-CT stage of porcelanite, whereas in accompanying calcareous sediments of the same age and thermal maturation level, quartz chert had formed. This led to speculations that, if the host rock is calcareous, opal-A might convert directly to quartz (quartz-precipitation hypothesis of Lancelot, 1973) without the intermediate opal-CT stage.

Experiments by Kastner *et al.* (1977) provided insight into the role of host-rock lithology and related solution chemistry for the opal-A to opal-CT transformation. These authors performed hydrothermal experiments reacting diatom frustules and radiolarian tests at 150°C with seawater or distilled water in in the presence of either calcareous ooze or montmorillonitic clay. The main results of these experiments can be summarized as follows:

1. In all experiments at 150°C, but not in all room-temperature experiments, corrosion of the siliceous tests took place after periods of one day to one month.
2. After 2 to 3 months, precipitation of opal-CT lepispheres was observed, but only in the experiments with seawater in the presence of calcite. In these experiments, *embryonic* opal-CT lepispheres could be detected after only one day. Precipitation of the lepispheres occurred preferentially on the surfaces of foraminifera.
3. In the presence of calcite, the concentration of dissolved silicon decreased compared with those without calcareous ooze, in which no opal-CT precipitation was observed.

Because of the known role of magnesium hydroxide as a coagulant in silica precipitation, particular attention was paid in these experiments on the effects of $Mg(OH)_2$ for the precipitation process. Apparently, the presence both of Mg-ions and hydroxyl-groups is essential for opal-CT crystallization, as shown by further results of Kastner *et al.* (1977):

4. In each of the experiments in which opal-CT crystallization occurred, the concentration of Mg^{2+} and $(OH)^-$ was lowered in the ratio 1:2, parallel with the decrease in the concentration of dissolved silicon.
5. Newly formed embryonic opal-CT lepispheres always contained trace amounts of Mg.
6. In the absence of Mg (*e.g.*, in experiments with artifical seawater lacking Mg), no opal-CT crystallization was observed during the experiment, even though calcite was present.
7. In experiments with initial borate alkalinity instead of bicarbonate alkalinity, opal-CT lepispheres formed in the same manner as in

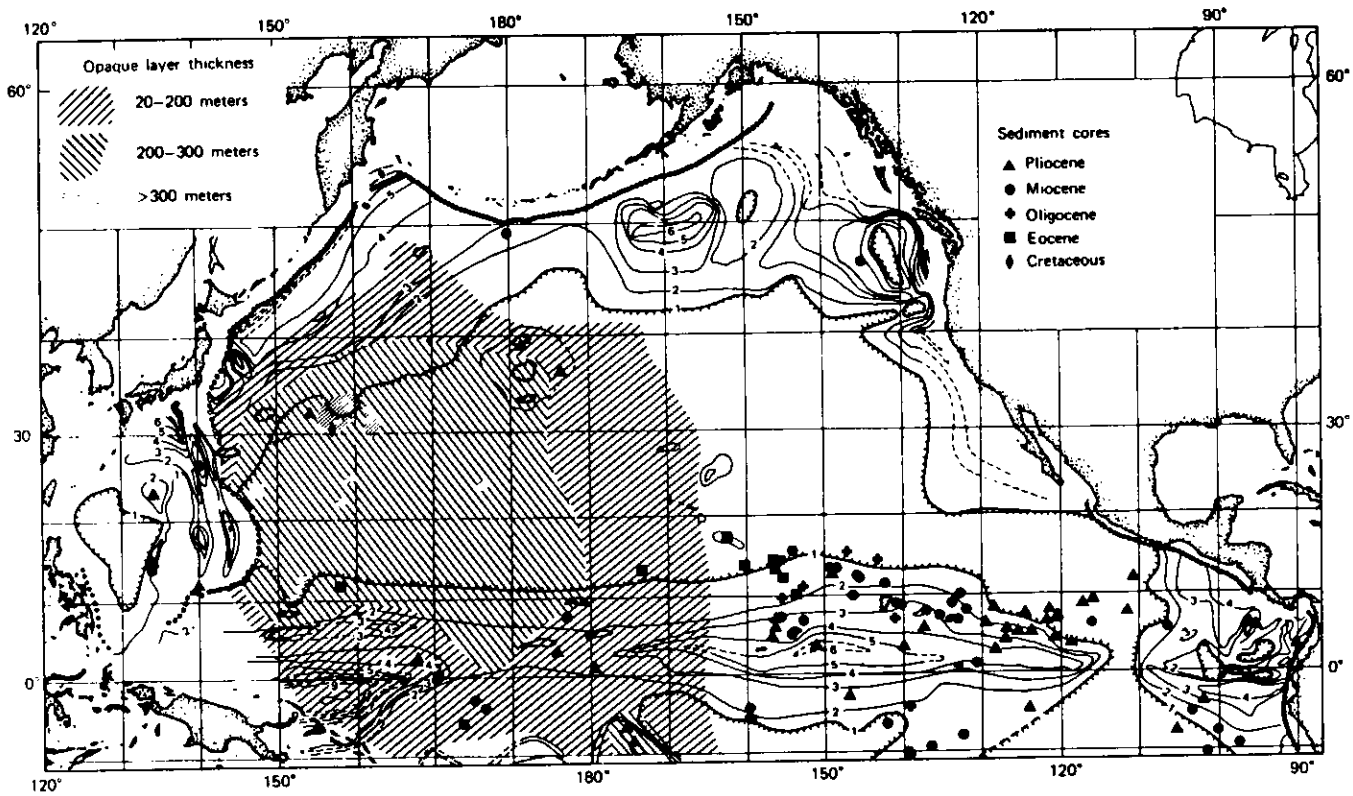

Figure 17 *Thickness of seismic-stratigraphic units in the Pacific (from Wyllie, 1971; after Ewing* et al., *1968). Isopach lines for upper transparent layer in tenths of seconds reflection time (two-way travel time, i.e., each contour represents approximately 100 m).*

the presence of bicarbonate indicating that it is the hydroxyl ion which is involved in the transformation and not the bicarbonate ion. 8. In experiments with montmorillonitic clays, dissolution of siliceous tests took place, but no reprecipitation of opal-CT occurred. However, small amounts of an Mg-rich clay formed.

The results highlighted the significance of a magnesium hydroxide compound (MHC) which attracts silanol groups with their high negative surface charge and causes them to precipitate and nucleate as opal-CT lepispheres. The MHC has been postulated to be the mineral sepiolite (Kent and Kastner, 1985). Opal-CT precipitation apparently is more rapid than sepiolite growth once the nuclei have formed, therefore opal-CT outdoes sepiolite. The role of calcium carbonate, which also dissolves in the process, is thought to resupply alkalinity consumed in the formation of the nuclei. Seawater supplies the necessary Mg. When the (OH)-groups have been exhausted, the rate of nucleus formation drops and the existing opal-CT embryos grow to well-developed lepispheres, (provided continued opal-A dissolution supplies the required dissolved silicon). In experiments with montmorillonitic clays, the clay minerals compete for the Mg and thus prevent the formation of the magnesium-hydroxide nuclei. Consequently, no opal-CT formed during the duration of the experiments (up to 6 months).

Opal-CT precipitation as rate-limiting factor. In a continuation of these hydrothermal experiments, Kastner and Gieskes (1983) determined the rate-limiting steps in the dissolution – reprecipitation process. The overall reaction rate is a function of the rates of dissolution, nucleation and growth of the silica phases involved. Which one of these mechanisms will be the rate-limiting factor depends on specific chemical and physical conditions. Amorphous silica of varying specific surface area was placed in aqueous solutions of $MgCl_2$ (0.03M) and $NaHCO_3$ (0.03M) and heated to temperatures of 50°, 75°, 100°, 125°, and 150°C for periods of 1 to 30 days (Figure 18). In all experiments, Mg and (OH) concentrations decreased in the 1:2 ratio previously established for the process, and opal-CT lepispheres or embryonic lepispheres formed. This confirmed that the MHC serves to nucleate the opal-CT. In experiments with low-surface-area silica (*i.e.*, Eocene *Radiolaria* with a specific surface area of 5.3 $m^2 \cdot g^{-1}$), the opal-A dissolution rate apparently was the rate- controlling step at temperatures of 50°, 75°, and 100°C. At these temperatures, the concentration of dissolved silicon remained below the equilibrium solubility of β-cristobalite, the silica phase which most closely approximates a "poorly ordered opal-CT" and for which solubility data are available. Nuclei formation and growth of opal-CT apparently kept pace with opal-A dissolution at these temperatures. At 125° and 150°C, however, opal-CT precipitation became the rate-limiting step after a few days, while the concentration of dissolved silicon rose above the equilibrium solubility of β-cristobalite (Figure 18). In experiments with higher-surface area silica (*i.e.*, Ludox

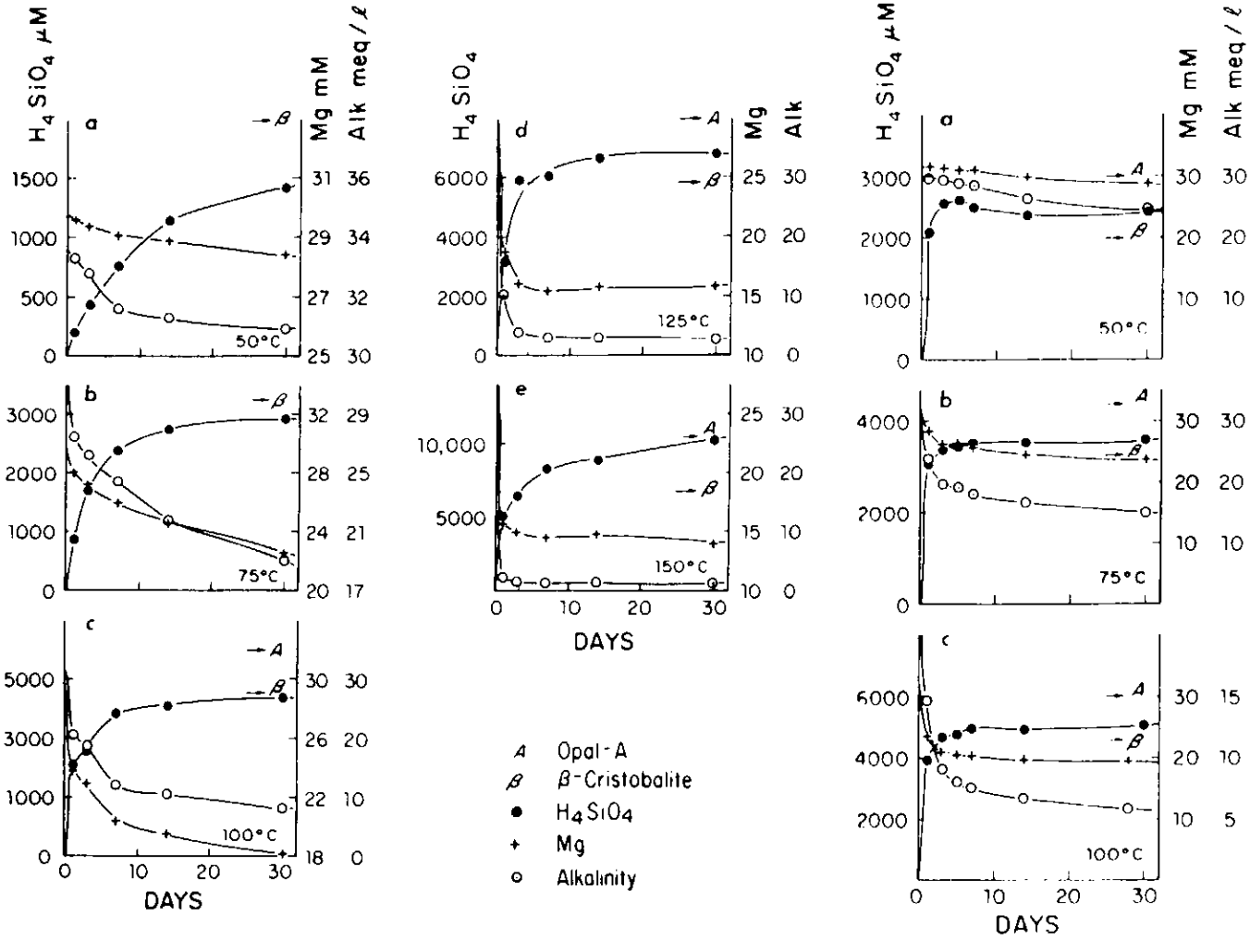

Figure 18 *Changes in dissolved silicon, magnesium and alkalinity as a function of time and temperature in hydrothermal experiments with Eocene Radiolaria (specific surface area of 5.3 $m^2 \cdot g^{-1}$). →β, solubility of β-crystobalite; →**A**, solubility of opal-A (from Kastner and Gieskes, 1983, fig. 1).*

Figure 19 *Changes as in Figure 18, however for Ludox silica (specific surface area of 61.5$m^2 \cdot g^{-1}$; from Kastner and Gieskes, 1983, fig. 2).*

silica with a specific surface area of 61.5 $m^2 \cdot g^{-1}$), the same behavior was found at all temperatures studied: β-cristobalite solubility was rapidly exceeded; but opal-A equilibrium solubility concentrations were not attained, again indicating that opal-CT precipitation was the rate-limiting process (Figure 19). These experiments also clearly illustrate the dominant role of temperature as rate-controlling factor in the conversion of opal-A to opal-CT.

The opal-CT to quartz transformation: Temperature and rate. Temperature estimates for the opal-CT to quartz transformation based on oxygen isotope data and heat-flow considerations for the Monterey Formation range from 55° to 110°C (Murata *et al.*, 1977; Murata and Larson, 1975; Pisciotto, 1981). The actual temperature at which the transformation occurs at a particular locality is a complex function of many factors, including the previous opal-CT maturation history. Pisciotto's (1981) temperature estimates for the base of the opal-CT zone in the Monterey Formation (35°-61°C), are also considerably lower than those of other authors as they were for the top of this zone.

As discussed previously, opal-CT precipitation is the rate-limiting factor in the opal-A to opal-CT conversion, when dissolution of immature, high-surface-area opal-A is involved. Under such conditions, the concentration of silicon in solution will eventually approach the theoretical equilibrium solubility value for opal-CT, which is a function of the surface area of this phase for a given temperature. Lowering the equilibrium solubility for dissolved silicon through Ostwald ripening of the opal-CT phase counterbalances a solubility increase with rising temperature during burial. This is a prerequisite for quartz precipitation. A high-surface-area opal-CT at 50°C has a theoretical solubility of 130 ppm. The solubility of a low-surface-area opal-CT at 110°C is about 150 ppm (Fournier, 1973), only slightly higher than that of the high-surface area opal-CT at 50°C. A solution "in equilibrium" with "ordered" opal-CT at 110°C, is therefore super-saturated only 1.5 times with respect to chalcedony or cryptocrystalline quartz. A solution "in equilibrium" with a high-surface-area (or "disordered") opal-CT at 110°C, on the other hand, would have a solubility of 290 ppm (Fournier, 1973) or nearly 3 times the equilibrium solubility of chalcedony. Since the growth of a new ("more highly ordered") silica phase such as chalcedony or quartz is favoured by low supersaturation, the "ordering" process during burial of opal-CT operates toward this end and ultimately facilitates quartz precipitation.

Lowered silicon concentrations are also required to understand the reduced *d*(101) spacing of the initial opal-CT in clayey host sediments. In the Monterey Formation, Isaacs (1982) observed that the first opal-CT to appear in a progressive burial sequence has a *d*(101) spacing which varies inversely with detrital mineral content of the host sediment (Figure 20). This observation confirms the results of Murata and Larson (1975) from the Chico Martinez Creek study that, at any given burial depth, the opal-CT d-spacing in (detritus-rich) porcelanite is 0.004-0.015 Å smaller than in associated (detritus-poor) quartz chert (Figure 12). This indicates *retardation of* opal-CT *nucleation* in clayey sediments because of the competition for MHC by clay minerals, consistent with the results of Kastner *et al.* (1977). Furthermore, it indicates *delayed growth* of opal-CT until silicon solubilities "in equilibrium" with a lower surface-area opal-CT (of a *d*-spacing of 4.08 Å or less) are encountered. Such reduced silicon concentrations in clay-rich host sediments can be accomplished most easily by adsorption of silica on detrital minerals (Siever and Woodford, 1973) and by the neoformation of silica-rich clay minerals, provided their nucleation and growth rates are faster than those of the silica phases that could potentially form. These and other possible scenarios are discussed in more detail by Williams *et al.* (1985).

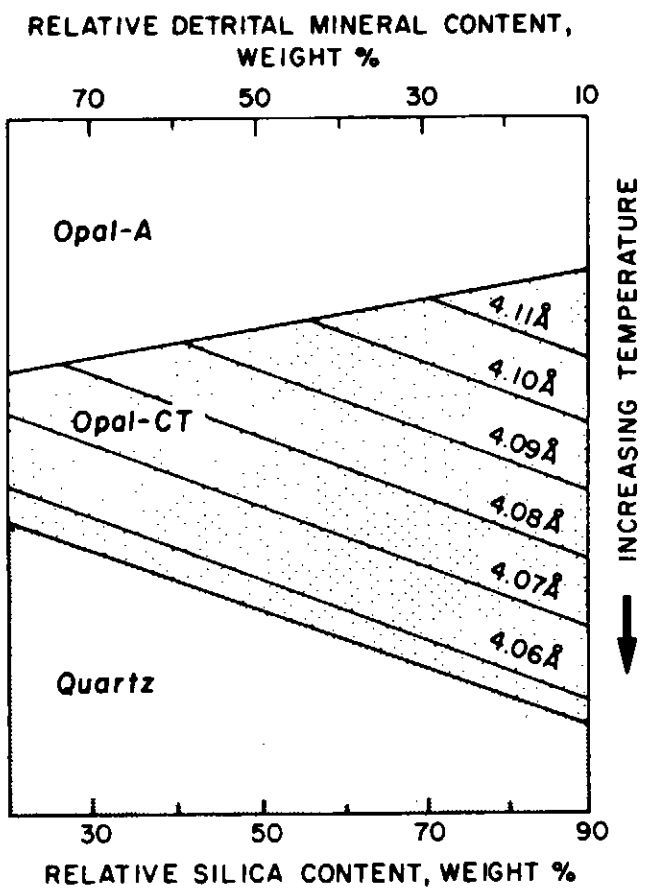

Figure 20 *Schematic summary of the role of host rock composition and temperature as controlling factors in the opal-CT maturation sequence. The initial d(101) spacing of opal-CT has been shown to vary inversely with detrital content. (From Isaacs* et al., *1983; after Isaacs, 1982).*

The findings of Isaacs (1982) summarized in Figure 20 also suggest that the detrital mineral content, while retarding the opal-A to opal-CT transformation, would actually enhance the opal-CT to quartz transformation, which is what one would expect from the discussion in the previous section. In sediments with more than 70% detrital minerals the initial opal-CT has a *d*(101) spacing of 4.08Å or less. In these sediments, the transformation to quartz should occur earlier than in sediments with less than 30% detrital minerals with an initial *d*(101) spacing of 4.11 Å. This is because reduction of the opal-CT *d*-spacing to values below 4.07Å (4.09Å in certain Cretaceous cherts from the West Pacific (Pisciotto, 1980)) is a prerequisite for quartz precipitation. Such an inference, however, is at variance with the earlier observation (*i.e.*, Lancelot, 1973) that the silica maturation sequence seems to be accelerated in calcareous host rocks, which leads to the relatively early formation of quartz chert.

This ambiguity might be resolved, if it is assumed that the initial retardation of the opal-A to opal-CT transformation in clayey sediments delays the entire silica maturation sequence to an extent which cannot be compensated for by later acceleration due to an abbreviated opal-CT stage. Although the opal-CT stage may in fact last longer in carbonates than in clay-rich siliceous sediments, contrary to Lancelot's (1973) assumption, this may be outweighed by a considerably earlier initiation of the transformation sequence in carbonates.

The field relationship between detrital content and opal-CT transformation rates

reported by Isaacs (1982) from the Santa Barbara coast is not observed everywhere in the Monterey Formation. Pisciotto (1981), for example, found the appearance of opal-CT as well as quartz at lower temperatures in the Santa Barbara basin to be associated with lower detritus contents. The most recent study of the problem by Hinman (1987) investigated the role of organic matter for the transformation reactions. Her results suggest that in organic-matter rich sediments the rate of silica diagenesis should be reduced. Organic acids released by organic-matter maturation would dissociate and lower the pH thereby reducing carbonate alkalinity. This in turn would slow down the transformations by decreasing the silica polymerization rate. Although lowering of the pH will promote carbonate dissolution and thus buffer the pH, this effect may be nullified, if little carbonate is available or accessible for dissolution. In this case, no effect of carbonate content on the silica transformation rates may be seen, as in Isaacs' (1982) study. The initial opal-CT formed in organic-matter rich sediments should have a lower *d*(101) spacing because of a slower nucleation and growth rate under decreased carbonate alkalinity. In so far as organic-matter content may be positively correlated with detrital mineral content, Hinman's (1987) results are in accordance with Isaacs' findings. However, Hinman (1987) did not find evidence that an initially lower *d*(101) spacing of opal-CT in organic-matter and detritus-rich sediments also accelerates the subsequent transition to quartz. In contrast, in the Santa Maria basin, quartz formation seemed to be slowed down because it occurred at higher temperatures in porcelanite than in chert.

It seems unlikely that the opal-CT stage can be bypassed entirely in the normal diagenetic silica maturation process, except under special conditions. The reasons why the diagenetic evolution path opal-A → opal-CT → quartz is observed in most situations have been outlined in the previous sections on reaction kinetics, and confirm the applicability of Ostwald's step-rule for diagenetic silica transformations. Rare exceptions seem to be restricted to micro-environments such as the cavities of foraminifera (*e.g.*, Keene, 1975) or Radiolaria in calcareous sediments. These are often filled with chalcedony, while the host rocks are calcareous opal-CT rocks or diatomaceous (opal-A) shales (Isaacs, 1982). This indicates anomalously early quartz (*i.e.*, chalcedony) precipitation. Precipitation of the chalcedony occurred in spherical open cavities indicating limited overburden weight and very shallow burial. This chalcedony does not appear to have had an opal-CT precursor in the cavities, because elsewhere in the host rock opal-CT is still present which shows no sign that the transformation to quartz has started. Most likely, the chalcedony formed directly from opal-A, possibly because the concentration of dissolved silicon in the microenvironment of the cavities, for some unknown reason, remained below α-cristobalite equilibrium solubility during the early stage of opal-A dissolution. Among the mechanisms discussed by Williams *et al.* (1985) to maintain low silica concentrations in pelagic carbonates, the early precipitation of calcium zeolites is a possibility, although it seems no specific studies have been directed at this problem.

Hinman (1987) suggested that direct quartz precipitation may be possible in the absence of Mg^{2+}, if sufficient alkalinity is available. Mg^{2+} ions in solution appear to have an inhibiting effect on quartz precipitation. This behaviour is opposite to that of opal-CT crystallization, which is promoted in the presence of Mg^{2+} (and high alkalinity).

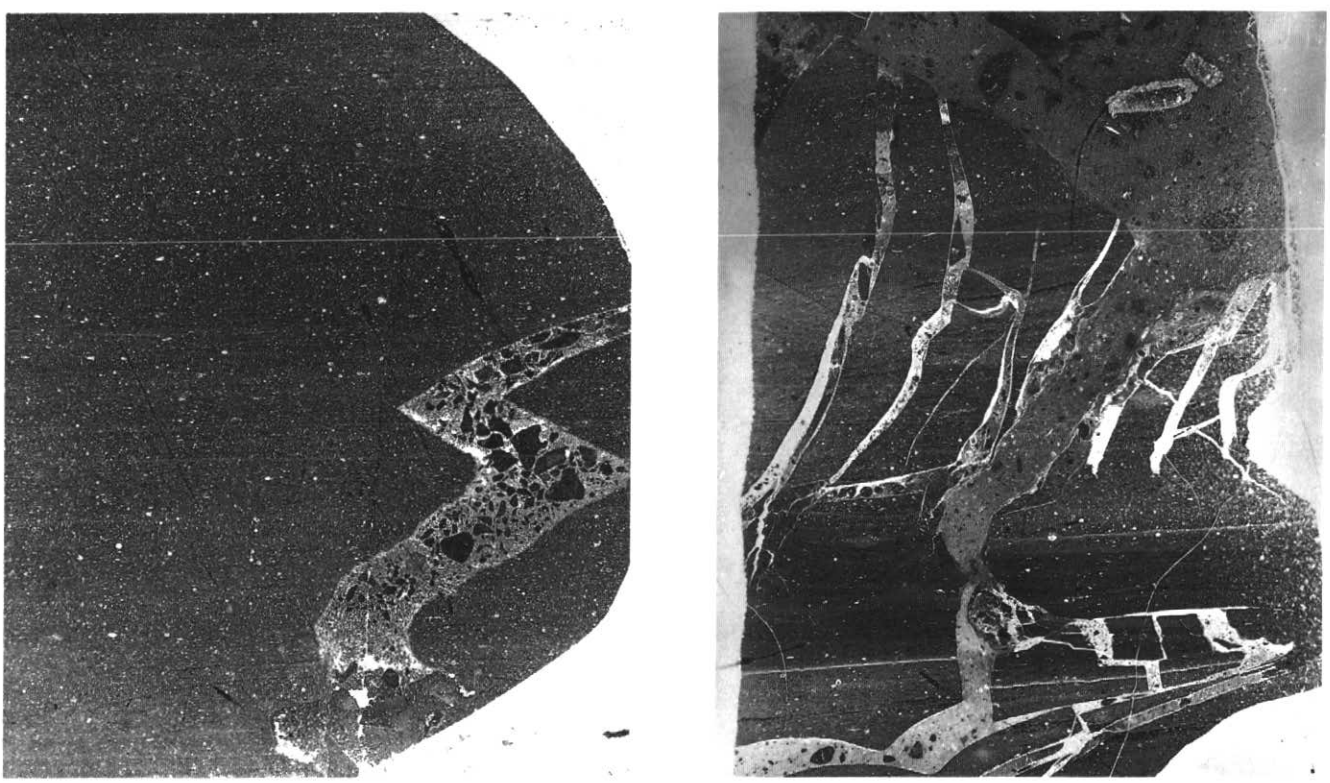

Figure 21 ***(a) (left)*** *Folded chert dyke in Lower Cretaceous radiolarian porcelanite, West Pacific. Porcelanite fragments in the dyke are cemented by microquartz and chalcedony which enclose considerable amounts of opal-CT sediment, except where the cement is very light-coloured (especially at the dyke margins). Folding of the microdyke was caused by differential compaction. The pure chalcedonic cement at the dyke margin was probably precipitated into pore space that was generated by shrinkage of the host sediment during ongoing compaction and was probably the latest cement phase. Height of thin-section approximately 2 cm. DSDP site 20-198A, sample 5cc, #1.*

(b) (right) *Multiple fractures filled with injected opal-CT sediment and fragments which were cemented by microquartz and chalcedony. Margins and ends of the finer fractures are light-coloured and consist almost entirely of microquartz or chalcedony cement which probably was the last cement. Height of section approximately 2.5 cm. DSDP site 20-198A, sample 5cc, #4.*

Summary: The "stability" fields of the various silica phases in deep-sea diagenetic environments. The distribution of the various silica phases in oceanic sediment sequences has been summarized by Riech and v. Rad (1979) on the basis of available DSDP data (Figure 16). There is considerable overlap on this depth/age graph between the fields for the three main silica phases.

Opal-A has been found in sediments as old as 85 m.y. (Late Cretaceous), but only at shallow subsurface depths. With increasing depth (and temperature) its maximum survival time is shortened significantly. For example, at 1,000 m subsurface depth, opal-A is normally no longer present in sediments older than about 20 m.y.

Opal-CT takes a minimum of about 10 m.y. to first appear, and this requires elevated heat-flow, otherwise its formation takes even longer. Exceptionally young opal-CT has been observed by Weaver and Wise (1973) in Pliocene sediments (less than 5 m.y.), where it occurred adjacent to igneous dykes and sills injected close to the sediment/water interface. On the other hand, opal-CT may still persist in sediments 100 to 120 m.y. old. Little new opal-CT forms, however, in pre-Tertiary sediments (*i.e.*, sediments older than 65 m.y.), because very little source material (opal-A) is left in those sediments. With age and increasing burial, opal-CT undergoes the progressive crystallographic structural changes in the *d*(101) spacing described earlier. No opal-CT has been found in pre-Cretaceous sediments (older than 144 m.y.).

In Figure 16, the quartz field overlaps the opal-CT field, and to a slight degree the opal-A field, illustrating how local variations in heat flow, pore fluid chemistry, host-rock lithology and other factors can affect the rate of the diagenetic transformations. Quartz cherts need a minimum of 30 to 40 m.y. to form at burial depths of 500 m or more, and considerably longer at shallower depths. Genuine quartz cherts, consequently, are rare in Cenozoic pelagic sediments, but become predominant in Lower Cretaceous and older siliceous rocks. They are the exclusive lithology of siliceous sediments in the Paleozoic and Precambrian.

Physical Diagenesis of Siliceous Sediments

The treatment of the diagenesis of siliceous sediments would be lacking an important aspect without a discussion of some phenomena of physical diagenesis in cherts. A step-wise compaction history is characteristic of siliceous sediments during burial, which contrasts with the more gradual compaction history of argillaceous sediments. This is implicit in the constant bulk density of Figure 12 for the opal-CT stage and reflects the rapid crystallographic changes associated with the phase changes at the stage boundaries.

Other diagenetic features characteristic of chert formations are dykes, diapirs, and breccias which have been well described in the literature (*e.g.*, Taliaferro, 1934). They attest to differential compaction and variable rates of silica recrystallization and cementation. In a given sequence of siliceous sediments, some layers may already be lithified or semi-lithified while others are not. Shaking during an earthquake may rupture the lithified layers and cause injection of unlithified sediment into the fractures from adjacent uncemented layers (see numerous illustrations in Snyder *et al.*, 1983), particularly if these had been overpressured. The opal-A to opal-CT and the opal-CT to quartz transformations are dehydration reactions. They may generate excess pore pressure and cause hydraulic fracturing. The examples shown in Figure 21 are Cretaceous radiolarian porcelanites from the West Pacific east of the Marianas deep-sea trench/island arc. The dykes probably reflect seismic activity associated with the Marianas subduction zone. The brittle host sediment is porcelanite predominantly consisting of opal-CT with chalcedony-filled radiolarians. The fractures and dykes contain porcelanite fragments and fine-grained opal-CT sediment cemented by microquartz and chalcedony. Some of the microquartz seems to have recrystallized in place from opal-CT. The folded dyke in Figure 21a behaved as a more competent layer, while the surrounding host sediment was still undergoing compaction. Similar mechanisms of dyke and vein formation are invoked by Steinitz (1970) and Snyder *et al.* (1983). Paris *et al.* (1985) ascribe chert breccias and veins in the Archean Barberton greenstone belt in South Africa to the injection of hot, high-pressure hydrothermal fluids related to volcanism. Some chert breccias, however, are of normal epigenetic, synsedimentary origin, such as the ones in the Burlington Limestone of Missouri which according to Carozzi and Gerber (1978) formed due to storm action on a Mississippian carbonate flat. They provide evidence for the early-diagenetic origin of some chert-nodules in limestones, which will be discussed in more detail in Hesse *(in press)*.

Conclusions

Our understanding of the origin of biogenic cherts, the main type of Phanerozoic cherts, has improved significantly during the last 15 years. Principal remaining open questions concern the mineralogical significance of the shift in the *d*(101)-spacing in opal-CT with maturation, which is closely related to the problem of solid-state reactions at low temperatures. To solve this problem, a better understanding of the crystallographic structure of the mineral opal-CT is required. The influence of host-rock lithology on the diagenetic silica transformations also requires further study. Results of Isaacs (1982) suggest that detrital content accelerates the opal-CT to quartz transformation while it has a retarding effect on the opal-A to opal-CT transformation (Kastner *et al.*, 1977). However, the overall maturation seems to be faster in carbonates than in clayey sediments (Lancelot, 1973).

Acknowledgements

Funding for this review and the author's research on diagenesis came from the Natural Sciences and Engineering Research Council of Canada. Valuable critical comments were provided by S. Calvert, E. McBride, A. Mucci and especially T. Barrett, which helped considerably to streamline the manuscript. U. v. Rad made available the originals for most of the photomicrographs included in this review. R. Yates helped with the photography and drafting. This support is gratefully acknowledged.

References

General *These cover the sections Introduction, Sources of non-detrital silica in siliceous sediments, Biogenic siliceous oozes, Pelagic stratigraphy, Formation of bedded chert, Shallow water chert, and Conclusions*

Baltuck, M., 1983, Some sedimentary and diagenetic signatures in the formation of bedded radiolarite, *in* Iijima, A., Hein, J.R. and Siever, R., eds., Siliceous Deposits in the Pacific Region: Developments in Sedimentology, v. 36, p. 299-315.

Barrett, T.J., 1981, Chemistry and mineralogy of Jurassic bedded chert overlying ophiolites in the North Apennines, Italy: Chemical Geology, v. 34, p. 289-317.

Bates, R.L. and Jackson, J.A., 1980, Glossary of geology, Second edition: American Geological Institute, Falls Church, Va., 749 p.

Berger, W.H., 1970, Biogenous deep-sea sediments: fractionation by deep-sea circulation: Geological Society of America, Bulletin, v. 81, p. 1385-1401.

Berger, W.H., and Winterer, E.L., 1974, Plate stratigraphy and the fluctuating carbonate line, *in* Hsü, K. and Jenkyns, H.C., eds., Pelagic sediments on land and under the sea: International Association of Sedimentologists, Special Publication, v. 1, p. 11-48.

Bosellini, A. and Winterer, E.L., 1975, Pelagic limestone and radiolarite of the Tethyan Mesozoic: A genetic model: Geology, v. 3, p. 279-282.

Bramlette, M.N., 1946, The Monterey Formation of California and the origin of its siliceous rocks: United States Geological Survey, Professional Paper 212, 55 p.

Calvert, S.E., 1966a, Accumulation of diatomaceous silica in the sediments of the Gulf of California: Geological Society of America, Bulletin, v. 77, p. 569-596.

Calvert, S.E., 1966b, Origin of diatom-rich sediments from the Gulf of California: Journal of Geology, v. 74, p. 546-565.

Calvert, S.E., 1968, Silica balance in the ocean and diagenesis: Nature, v. 219, p. 919-920.

Calvert, S.E., 1983, Sedimentary geochemistry of silicon, *in* Aston, S.R., ed., Silicon Geochemistry and Biogeochemistry: New York, Academic Press, p. 143-186.

Carver, R.E., 1980, Petrology of Paleocene-Eocene and Miocene opaline sediments, southeastern Atlantic coastal plain: Journal of Sedimentary Petrology, v. 50, p. 569-582.

Cavaroc, V.V., Jr and Ferm, J.C., 1968, Siliceous spiculites as shoreline indicators in deltaic sequences: Geological Society of America, Bulletin, v. 79, p. 263-271.

Chipping, D.H., 1971, Paleoenvironmental significance of chert in the Franciscan Formation of western California: Geological Society of America, Bulletin, v. 82, p. 1707-1712

Dapples, E.C., 1967, Silica as an agent in diagenesis, *in* Larsen, G. and Chilingar, G.V., eds., Diagenesis in sediments. Developments in Sedimentology, v. 8, p. 323-342.

DeMaster, D.J., 1981, The supply and accumulation of silica in the marine environment: Geochimica et Cosmochemica Acta, v. 45, p. 1715-1732

Diersche, V., 1980, Die Radiolarite des Oberjura im Mittelabschnitt der Nordlichen Kalkalpen: Geotektonische Forschungen, v. 58, 217 p.

Edmond, J.M., Measures, C., McDuff, R.E., Chan, L.H., Collier, R., Grant, B., Gordon, L.I. and Corliss, J.B., 1979a, Ridge crest hydrothermal activity and the balances of the major and minor elements in the ocean: The Galapagos data: Earth and Planetary Science Letters, v. 46, p. 1-18.

Edmond, J.M., Jacobs, S.S., Gordon, A.L., Mantyla, A.W. and Weiss, R.F., 1979b, Water column anomalies in dissolved silica over opaline pelagic sediments and the origin of the deep silica maximum. Journal of Geophysical Research, v. 84 (C12), p. 7809-7826.

Folk, R.L. and McBride, E.F., 1978, Radiolarites and their relation to subjacent "oceanic crust" in Liguria, Italy: Journal of Sedimentary Petrology, v. 48, p. 1069-1101.

Garrels, R.M., 1987, A model for the deposition of the microbanded Precambrian iron formations: American Journal of Science, v. 287, p. 81-96.

Gibson, T.G. and Towe, K.M., 1971, Eocene volcanism and the origin of the horizon A: Science, v. 172, p. 154-154.

Goldstein, A., Jr., 1959, Cherts and novaculites of Ouachita facies, *in* Ireland, H.A., ed., Silica in Sediments: Society of Economic Paleontologists, Special Publication, No. 7, p. 135-149.

Griffin, J., 1980, The effect of pressure on the solubility of 11 silicates in seawater at 20°C, pH 8: Unpublished M.Sc. thesis, University of Hawaii, Honolulu.

Heath, G.R., 1969, Mineralogy of Cenozoic deep-sea sediments from the equatorial Pacific Ocean: Geological Society of America, Bulletin, v. 80, p. 1997-2018.

Heath, G.R., 1974, Dissolved silica and deep-sea sediments, *in* Hay, W.W., ed., Studies in Paleo-oceanography: Society of Economic Paleontologists and Mineralogists, Special Publication, v. 20, p. 77-93.

Hein, J.R. and Karl, S.M., 1983, Comparisons between open-ocean and continental margin chert sequences, *in* Iijima, A., Hein, J.R. and Siever, R., eds., Siliceous deposits in the Pacific Region. Developments in Sedimentology, v. 36, p. 25-43.

Hesse, R., *in press*, Origin of chert: II. Diagenesis of inorganic and replacement cherts, *in* McIlreath, I. and Morrow, D., eds., Diagenesis: Geological Association of Canada, Geoscience Canada Reprint Series 4.

Hesse, R., Foreman, H.P., Forristall, G.Z., Heezen, B.C., Hekel, H., Hoskins, R.H., Jones, E.J.W., Kaneps, A.G., Krashenninikov, V.A., MacGregor, I. and Okada, H., 1974, Walther's facies rule in pelagic realm, a large-scale example from the Mesozoic-Cenozoic Pacific: Zeitschrift der Deutschen Geologischen Gesellschaft, v. 125, p. 151-172.

Hurd, D.C., 1973, Interactions of biogenic opal, sediment and seawater in the central Equatorial Pacific: Geochimica et Cosmochimica Acta, v. 37, p. 2257-2282.

Hurd, D.C., 1983, Physical and chemical properties of siliceous skeletons, *in* Aston, S.R., ed., Silicon Geochemistry and Biogeochemistry: Academic Press, New York, p. 187-244.

Imoto, N. and Saito, Y., 1973, Scanning electron microscopy of chert: Bulletin of the Natural Science Museum (Tokyo), v. 16, p. 397-400

Imoto, N., Shimizu, D., Shiki, T. and Yoshida, M., 1974, Sole markings observed in bedded cherts from the Tamba belt, Southwest Japan: Bulletin Kyoto University of Education, v. B44, p. 19-26 (in Japanese)

Isaacs, C.M., 1982, Influence of rock composition on kinetics of silica phase changes in the Monterey Formation, Santa Barbara area, California: Geology, v. 10, p. 304-308.

Isaacs, C.M., 1984, The Monterey - key to offshore California boom: Oil and Gas Journal, v. 82, p. 75-81

Isaacs, C.M., Pisciotto, K.A. and Garrison, R.E., 1983, Facies and diagenesis of the Miocene Monterey Formation, California: A summary, *in* Iijima, A., Hein, J.R. and Siever, R., eds., Siliceous Deposits in the Pacific Region: Developments in Sedimentology, v. 36, p. 247-282.

Jenkyns, H.C and Winterer, E.L., 1982, Palaeoceanography of Mesozoic ribbon radiolarites. Earth and Planetary Science Letters, v. 60, p. 351-375.

Jones, D.L. and Murchey, B., 1986, Geologic significance of Paleozoic and Mesozoic radiolarian chert: Annual Reviews of Earth and Planetary Sciences, v. 14, p. 455-492.

Kastner, M., Keene, J.B. and Gieskes, J.M., 1977, Diagenesis of siliceous oozes. I. Chemical controls on the rate of opal-A to opal-CT transformation - an experimental study. Geochimica et Cosmochimica Acta, v. 41, p. 1041-1059.

Lancelot, Y., 1973, Chert and silica diagenesis in sediments from the central Pacific, *in* Winterer, E.L., Ewing, J.I., *et al.*, Initial Reports of the Deep Sea Drilling Project, v. 17, p. 377-405: United States Government Printing Office, Washington, D.C.

Lane, N.G., 1981, A nearshore sponge spicule mat from the Pennsylvanian of west-central Indiana: Journal of Sedimentary Petrology, v. 51, p. 197-202.

McBride, E.F. and Folk, R.L., 1979, Features and origin of Italian Jurassic radiolarites deposited on continental crust: Journal of Sedimentary Petrology, v. 49, p. 837-868.

Mizutani, S. and Shibata, K., 1983, Diagenesis of Jurassic siliceous shale in central Japan, *in* Iijima, A., Hein, J.R. and Siever, R., eds., Siliceous Deposits in the Pacific Region: Developments in Sedimentology, v. 36, p. 283-298.

Nisbet, E.G. and Price, I., 1974, Siliceous turbidites: bedded cherts as redeposited ocean ridge-derived sediments, *in* Hsü, K. and Jenkyns, H.C., eds., Pelagic sediments on land and under the sea: International Association of Sedimentologists, Special Publication, v. 1, p. 351-366.

Robertson, A.H.F., 1977, The origin and diagenesis of cherts from Cyprus: Sedimentology, v. 24, p. 11-30.

Sano, H., 1983, Bedded cherts associated with greenstones in the Sawadani and Shimantogawa Groups, Southwest Japan, *in* Iijima, A., Hein, J.R. and Siever, R., eds., Siliceous Deposits in the Pacific Region: Developments in Sedimentology, v. 36, p. 427-440.

Schmid, F., 1986, Flint stratigraphy and its relationship to archeology, *in* Sieveking, G. de G. and Hart, M.B., eds., The scientific study of flint and chert, Cambridge, Cambridge University Press, p. 1-5.

Steinberg, M., Bonnot-Courtois, C. and Tlig, S., 1983, Geochemical contribution to the understanding of bedded chert, *in* Iijima, A., Hein, J.R. and Siever, R., eds., Siliceous Deposits in the Pacific Region: Developments in Sedimentology, v. 36, p. 193-210.

Steinmann, G., 1906, Geologische Beobachtungen in den Alpen II: Die Schardtsche Überfaltungstheorie und die geologische Bedeutung der Tiefseeabsätze und der ophiolitischen Massengesteine: Berichte der Naturforschenden Gesellschaft Freiburg, v. 16, p. 18-67.

Steinmann, G., 1927, Die ophiolithischen Zonen in den Mediterranen Kettengebirgen: Congrès Géologique International, Comptes Rendues, 14e session, Madrid, 1926, v. 2, p. 637-668

Weaver, C.E. and Beck, K.C., 1977, Miocene of the S.E. United States: a model for chemical sedimentation in a peri-marine environment: Sedimentary Geology, v. 17, p. 1-234.

Weaver, F.M. and Wise, S.W., 1974, Opaline sediments of the southeastern coastal plain and horizon A: Biogenic origin. Science, v. 184, p. 899-901.

Wenk, E., 1949, Die Assoziation von Radiolarienhornsteinen mit ophiolithischen Erstarrungsgesteinen als petrogenetisches Problem: Experientia, v. 5, p. 226-232.

Wermund, E.G. and Moiola, R.J., 1966, Opal, zeolites, and clays in an Eocene neritic bar sand: Journal of Sedimentary Petrology, v. 36, p. 248-253.

Wise, S.W. and Weaver, F.M., 1973, Origin of cristobalite-rich Tertiary sediments in the Atlantic and Gulf Coastal Plains: Transactions Gulf Coast Association of Geological Societies, v. 23, p. 305-323.

Stages of Burial Diagenesis in Biogenic Siliceous Sediments - Characteristics of the Silica Phases in Siliceous Sediments

Bramlette, M.N., 1946, The Monterey Formation of California and the origin of its siliceous rocks: United States Geological Survey, Professional Paper 212, 55 p.

Calvert, S.E., 1971, Composition and origin of North Atlantic deep sea cherts: Contributions to Mineralogy and Petrology, v. 33 p. 273-288.

Calvert, S.E., 1983, Sedimentary geochemistry of silicon, *in* Aston, S.R., ed., Silicon Geochemistry and Biogeochemistry: New York, Academic Press, p. 143-186.

Carver, R.E., 1980, Petrology of Paleocene-Eocene and Miocene opaline sediments, southeastern Atlantic Coastal Plain: Journal of Sedimentary Petrology, v. 50, p. 569-582.

Darragh, P.J., Gaskin, A.J. and Sanders, J.V., 1976, Opals: Scientific American, v. 264, p. 84-94.

Ernst, W.G. and Calvert, S.E., 1969, An experimental study of the recrystallization of porcelanite and its bearing on the origin of some bedded cherts: American Journal of Science, v. 267A, p. 114-133.

Flörke, O.W., Hollmann, R., v. Rad, U. and Rösch, H., 1976, Inter-growth and twinning in opal-CT lepispheres: Contributions to Mineralogy and Petrology, v. 58, p. 235-242.

Hurd, D.C. and Theyer, F., 1975, Changes in the physical and chemical properties of biogenic silica from the central Equatorial Pacific. 1. Solubility, specific surface area, and solution rate constants of acid-cleaned samples: Analytical Methods in Oceanography, American Chemical Society, Advances in Chemistry Series, v. 147, p. 211-230.

Iler, R.K., 1955, The colloid chemistry of silica and silicates: Cornell University Press, Ithaca, N.Y., 324 p.

Iler, R.K., 1973, Effect of adsorbed alumina on the solubility of amorphous silica in water: Journal of Colloid and Interface Science, v. 43, p. 399-408.

Iler, R.K., 1979, Chemistry of Silica: Wiley-Interscience, New York, 866 p.

Isaacs, C.M., Pisciotto, K.A. and Garrison, R.E., 1983, Facies and diagenesis of the Miocene Monterey Formation, California: A summary, *in* Iijima, A., Hein, J.R. and Siever, R., eds., Siliceous Deposits in the Pacific region: Developments in Sedimentology, v. 36, p. 247-282.

Jones, D.L. and Knauth, L.P., 1979, Oxygen isotopic and petrographic evidence relevant to the origin of the Arkansas Novaculite: Journal of Sedimentary Petrology, v. 49, p. 581-597.

Jones, J.B. and Segnit, E.R., 1971, The nature of opal. 1. Nomenclature and constituent phases: Journal of the Geological Society of Australia, v. 18, p. 57-68.

Krauskopf, K.B., 1956, Dissolution and precipitation of silica at low temperatures: Geochimica et Cosmochimica Acta, v 10, p. 1-26.

Lancelot, Y., 1973, Chert and silica diagenesis in sediments from the central Pacific, *in* Winterer, E.L., Ewing, J.I., *et al*, Initial Reports of the Deep Sea Drilling Project, v 17, p. 377-405 United States Government Printing Office, Washington, D.C.

Lewin, J., 1961, The dissolution of silica from diatom walls: Geochimica et Cosmochimica Acta, v. 21, p. 182-198.

Mallard, M.E., 1890, Sur la lussatite, nouvelle variete minerale cristallisee de silice: Bulletin de la Société française de Minéralogie et Cristallographie, v. 13, p. 63-66.

Meyers, W.J., 1977, Chertification in the Mississippian Lake Valley Formation, Sacramento Mountains, New Mexico: Sedimentology, v. 24, p. 75-105.

Parks, G.A., 1965, The isoelectric points of solid oxides, solid hydroxides, and aqueous complex systems: Chemical Reviews, v. 65, p. 177-198.

Pisciotto, K.A., 1981, Distribution, thermal histories, isotopic compositions and reflection characteristics of siliceous rocks recovered by the Deep Sea Drilling Project, *in* Warme, J.E., Douglas, R.G. and Winterer, E.L., eds., The Deep Sea Drilling Project: A decade of progress: Society of Economic Paleontologists and Mineralogists, Special Publication 32, p. 129-147.

Riech, V. and v. Rad, U., 1979, Silica diagenesis in the Atlantic Ocean: Diagenetic potential and transformations, *in* Talwani, M., Hay, W. and Ryan, W.B.F., eds., Deep drilling results in the Atlantic Ocean: Continental margins and paleoenvironment: American Geophysical Union, Maurice Ewing Series, v. 3, p. 315-341.

Tada, R. and Iijima, A., 1983, Identification of mixtures of opaline silica phases and its implication for silica diagenesis, *in* Iijima, A., Hein, J.R. and Siever, R., eds., Siliceous Deposits in the Pacific Region: Developments in Sedimentology, v. 36, p. 229-245.

Van Lier, J.A., De Bruyn, P.L. and Overbeek, J.T.G., 1960, The solubility of quartz: Journal of Physical Chemistry, v. 64, p. 1675-1682.

Volosov, A.G., Khodarovskiy, I.L. and Ryzhenko, B.N., 1972, Equilibria in the system SiO_2 - H_2O at elevated temperatures along the lower three-phase curve: Geochemistry International, v. 9, p. 362-377.

v. Rad, U., Riech, V. and Rösch, H., 1977, Silica diagenesis in continental margin sediments off Northwest Africa, *in* Lancelot, Y., Seibold, E., *et al.*, Initial Reports of the Deep Sea Drilling Project, v. 41, p. 879-905: United States Government Printing Office, Washington, D.C.

Walther, J.V. and Helgeson, H.C., 1977, Calculation of the thermodynamic properties of aqueous silica and the solubility of quartz and its polymorphs at high pressures and temperatures: American Journal of Science, v. 277, p. 1315-1351.

Weaver, F.M., and Wise, S.W., Jr., 1972, Ultramorphology of deep sea cristobalitic chert: Nature, Physical Science, v. 237, p. 56-57.

Williams, L.A. and Crerar, D.A., 1985, Silica diagenesis, II. General mechanisms: Journal of Sedimentary Petrology, v. 55, p. 312-321.

Williams, L.A., Parks, G.A. and Crerar, D.A., 1985, Silica diagenesis, I. Solubility controls: Journal of Sedimentary Petrology, v. 55, p. 301-311.

Wise, S.W., Jr., Buie, B.F. and Weaver, F.M., 1972, Chemically precipitated sedimentary cristobalite and the origin of chert: Eclogae Geologicae Helvetiae, v. 65, p. 157-163.

Nature of the Diagenetic Transformation Mechanisms between Different Silica Phases and Physical Diagenesis of Siliceous Sediments

Berger, W.H. and v. Rad, U., 1972, Cretaceous and Cenozoic sediments from the Atlantic Ocean, *in* Hayes, D.E., Pimm, A.C., *et al*, Initial Reports of the Deep Sea Drilling Project, v. 14, p. 787-954: United States Government Printing Office, Washington, D.C.

Bramlette, M.N., 1946, The Monterey Formation of California and the origin of its siliceous rocks: United States Geological Survey Professional Paper, v. 212, 55 p.

Carozzi, A.V. and Gerber, M.S., 1978, Synsedimentary chert breccia: A Mississippian tempestite: Journal of Sedimentary Petrology, v. 48, p. 705-708.

Christian, J.W., 1965, The theory of transformations in metals and alloys: Pergamon Press, Oxford, 975 p.

Clayton, R.N., O'Neil, J.R. and Mayeda, T.K., 1972, Oxygen isotope exchange between quartz and water: Journal of Geophysical Research, v. 77, p. 3057-3067.

Ewing, J., Ewing, M., Aitken, T. and Ludwig, W.J., 1968, North Pacific sediment layers measured by seismic profiling, *in* Knopoff, L., Drake, C.L. and Hart, P.J., eds., The crust and upper mantle of the Pacific area: American Geophysical Union, Geophysical Monograph, v. 12, p. 147-173.

Fournier, R.O., 1973, Silica in thermal waters: Laboratory and field investigations, *in* Ingerson, E., ed., International Symposium on Hydrogeochemistry and Biogeochemistry, Proceedings, Tokyo 1970: Clarke Co., Washington, D.C. v. 1 (Hydrogeochemistry), p. 122-139.

Griffin, J.J., Koide, M., Hohndorf, A., Hawkins, J.W. and Goldberg, E.D., 1972, Sediments of the Lau Basin - rapidly accumulating volcanic deposits: Deep-Sea Research, v. 19, p 139-148

Harrison, W.E., Hesse, R. and Gieskes, J.M., 1982, Relationship between sedimentary facies and interstitial water chemistry in slope, trench and Cocos plate sites from the Mid-America Trench transect, active margin off Guatemala, Leg 67, DSDP, *in* Huene, R., Aubouin, J., *et al.*, Initial Reports of the Deep Sea Drilling Project, v. 67, p. 603-614: United States Government Printing Office, Washington, D.C.

Heath, G.R., 1969, Mineralogy of Cenozoic deep-sea sediments from the equatorial Pacific Ocean: Geological Society of America, Bulletin, v. 80, p. 1997-2018.

Heath, G.R. and Moberly, R., Jr., 1971, Cherts from the western Pacific, Leg 7, Deep Sea Drilling Project, *in* Winterer, E.L., Riedel, W.R., *et al.*, Initial Reports of the Deep Sea Drilling Project, v. 7, p. 991-1007: United States Government Printing Office, Washington, D.C.

Hein, J.R., Scholl, D.W., Barron, J.A., Jones, M.J. and Miller, J., 1978, Diagenesis of late Cenozoic diatomaceous deposits and formation of the bottom simulating reflector in the southern Bering Sea: Sedimentology, v. 25, p. 155-181.

Hesse, R., 1987, Selective and reversible carbonate-silica replacements in Lower Cretaceous carbonate-bearing turbidites of the Eastern Alps: Sedimentology, v 34, p. 1055-1077

Hesse, R., Lebel, J. and Gieskes, J.M., 1985, Interstitial water chemistry of gas hydrate bearing sections on the Middle-America Trench Slope, Deep Sea Drilling Project, Leg 84, *in* Auboin, J., Huene, R.V., *et al*. Initial Reports of the Deep Sea Drilling Project, v. 84, p. 727-737: United States Government Printing Office, Washington, D.C.

Hinman, N.W., 1987, Organic and inorganic chemical controls on the rates of silica diagenesis: A comparison of a natural system with experimental results: Unpublished Ph D. thesis, University of California, San Diego, 381 p.

Hurd, D.C., Wenkham, C., Pankratz, H.S. and Fugate, J., 1979, Variable porosity in siliceous skeletons: Determination and importance: Science, v. 203, p. 1340-1343.

Iler, R.K., 1979, Chemistry of silica: Wiley-Interscience, New York, 866 p.

Isaacs, C.M., 1982, Influence of rock composition on kinetics of silica phase changes in the Monterey Formation, Santa Barbara area, California: Geology, v. 10, p. 304-308.

Kastner, M. and Gieskes, J.M., 1983, Opal-A to opal-CT transformation: A kinetic study, *in* Iijima, A., Hein, J.R. and Siever, R., eds., Siliceous deposits in the Pacific region: Developments in Sedimentology, v. 36, p. 211-227

Kastner, M., Keene, J.B., and Gieskes, J.M., 1977, Diagenesis of siliceous oozes. I. Chemical controls on the rate of opal-A to opal-CT transformation - an experimental study: Geochimica et Cosmochimica Acta, v. 41, p. 1041-1059.

Keene, J.B., 1975, Cherts and porcelanites from the North Pacific, DSDP, leg 32, *in* Larsen, R., Moberly, R., *et al.*, Initial Reports of the Deep Sea Drilling Project, v. 32, p. 429-507: United States Government Printing Office, Washington, D.C.

Keller, W.D., Stone, C.G. and Hoersch, W.D., 1985, Textures of Paleozoic chert and novaculite in the Ouachita Mountains of Arkansas and Oklahoma and their geological significance: Geological Society of America, Bulletin, v. 96, p. 1353-1363.

Kent, D.B. and Kastner, M., 1985, Mg^{2+} removal in the system Mg^{2+} - amorphous SiO_2 - H_2O by adsorption and Mg-hydroxysilicate precipitation: Geochimica et Cosmochimica Acta, v. 49, p. 1123-1136.

Labeyrie, L.D., 1974, New approach to surface seawater paleotemperatures using $^{18}O/^{16}O$ ratios in silica of diatom frustules: Nature, v. 248, p. 40-42.

Lancelot, Y., 1973, Chert and silica diagenesis in sediments from the central Pacific, *in* Winterer, E.L., Ewing, J.I., *et al.*, Initial Reports of the Deep Sea Drilling Project, v. 17, p. 377-405: United States Government Printing Office, Washington, D.C.

Mizutani, S., 1977, Progressive ordering of cristobalitic silica in the early stage of diagenesis: Contributions to Mineralogy and Petrology, v. 61, p. 129-140.

Morse, J.W., 1988, Paragenesis of sedimentary minerals and the Ostwald Step Rule: An irreversible thermodynamic approach: American Journal of Science, (in press).

Murata, K.J., Friedman, I. and Gleason, J.D., 1977, Oxygen isotope relations between diagenetic silica minerals in Monterey Shale, Temblor Range, California: American Journal of Science, v. 277, p. 259-272.

Murata, K.J. and Larson, R.R., 1975, Diagenesis of Miocene siliceous shales, Temblor Range, California: United States Geological Survey, Journal of Research, v. 3, p. 553-566.

Murata, K.J. and Norman, M.B., II, 1976, An index of crystallinity for quartz: American Journal of Science, v. 276, p. 1120-1130.

Murata, K.J. and Randall, R.G., 1975, Silica mineralogy and structure of the Monterey Shale, Temblor Range, California: United States Geological Survey, Journal of Research, v. 3, p. 567-572.

Nielsen, A.E., 1964, Kinetics of precipitation: The Macmillan Co., New York, 151 p.

Paris, I., Stanistreet, I.G. and Hughes, M.J., 1985, Cherts of the Barberton greenstone belt interpreted as products of submarine exhalative activity: Journal of Geology, v. 93, p. 111-129.

Pisciotto, K.A., 1980, Chert and porcellanite from Deep Sea Drilling Project Site 436, Northwest Pacific, *in* Langseth, M., Okada, H., *et al.*, Initial Reports of the Deep Sea Drilling Project, v. 56/57, p. 1133-1142. United States Government Printing Office, Washington, D.C.

Pisciotto, K.A., 1981, Diagenetic trends in the siliceous facies of the Monterey Shale in the Santa Maria region, California: Sedimentology, v. 28, p. 547-571.

Siever, R. and Woodford, N., 1973, Sorption of silica by clay minerals: Geochimica et Cosmochimica Acta, v. 37, p. 1851-1880

Snyder, W.S., Brueckner, H.K. and Schweikert, R.A., 1983, Deformational styles in the Monterey Formation and other siliceous rocks, *in* Isaacs, C.M. and Garrison, R., eds., Symposium volume on Monterey oilfields: Society of Economic Paleontologists and Mineralogists, Pacific Section, Los Angeles, p. 151-170

Stein, C.L. and Kirkpatrick, R.J., 1976, Experimental porcelanite recrystallization kinetics: A nucleation and growth model: Journal of Sedimentary Petrology, v. 46, p. 430-435.

Steinitz, G., 1970, Chert "dike" structures in Senonian chert beds, southern Negev, Israel: Journal of Sedimentary Petrology, v. 40, p. 1241-1254.

Taliaferro, N.L., 1934, Contraction phenomena in cherts: Geological Society of America, Bulletin, v. 45, p. 189-231.

Van Lier, J.A., de Bruyn, P.L. and Overbeek, J.T.G., 1960, The solubility of quartz: Journal of Physical Chemistry, v. 64, p. 1675-1682

v. Rad, U., 1979, SiO_2 - Diagenese in Tiefsee-sedimenten: Geologische Rundschau, v. 68, p. 1025-1036

v. Rad, U. and Rösch, H., 1972, Mineralogy and origin of clay minerals, silica and authigenic silicates in leg 14 sediments, *in* Hayes, D.E., Pimm, A.C., *et al.*, Initial Reports of the Deep Sea Drilling Project, v. 14, p. 727-751 United States Government Printing Office, Washington, D.C.

Weaver, F.M. and Wise, S.W., Jr., 1972, Ultramorphology of deep sea cristobalitic chert: Nature, v. 237, p. 56-57.

Weaver, F.M. and Wise, S.W., Jr., 1973, Early diagenesis of a deep see bedded chert: United States Antarctic Journal, v. 8, p. 298-300.

Williams, L.A. and Crerar, D.A., 1985, Silica diagenesis, II: General mechanisms: Journal of Sedimentary Petrology, v. 55, p. 312-321.

Williams, L.A., Parks, G.A. and Crerar, D.A., 1985, Silica diagenesis, I. Solubility controls: Journal of Sedimentary Petrology, v. 55, p. 301-311.

Wise, S.W., Jr., Buie, B.F. and Weaver, F.M., 1972, Chemically precipitated sedimentary cristobalite and the origin of chert: Eclogae Geologicae Helvetiae, v. 65, p. 157-163.

Wyllie, P.J., 1971, The dynamic earth: Textbook in geosciences: Wiley-Interscience, New York, 476 p.

Zemmels, I. and Cook, H.E., 1973, X-ray mineralogy from the Central Pacific Ocean, *in* Winterer, E.L., Ewing, J.I., *et al.*, Initial Reports of the Deep Sea Drilling Project, v. 17, p. 517-559: United States Government Printing Office, Washington, D.C.

Accepted, as revised, 26 July 1988.